Mixed states in ferromagnetic superconductors

H. Matsumoto, R. Teshima, and H. Umezawa
Theoretical Physics Institute, The University of Alberta, Edmonton, Alberta T6G 2J1, Canada

M. Tachiki
The Research Institute for Iron, Steel and Other Metals, Tohoku University, Katahina, Sendai 980, Japan

(Received 24 November 1981; revised manuscript received 20 September 1982)

A detailed study of the mixed state of the ferromagnetic rare-earth compounds $R\mathrm{Rh}_4\mathrm{B}_4$, $R_x\mathrm{Mo}_6\mathrm{S}_8$, and $R_x\mathrm{Mo}_6\mathrm{Se}_6$ is presented. The saturation effect of the magnetic moments is taken into account. Depending on the parameters, there are many types of phase transitions between the type-II/2, type-II/1, and type-I mixed states and the paramagnetic Meissner state, ferromagnetic Meissner state, spin-periodic Meissner state, and the self-induced vortex state. It is predicted that the magnetization can exhibit a variety of unusual modes.

I. INTRODUCTION

The discovery of the magnetic transition from the superconducting state to the ferromagnetic state in $\mathrm{ErRh}_4\mathrm{B}_4$ (Ref. 1) and $\mathrm{Ho}_{1.2}\mathrm{Mo}_6\mathrm{S}_8$ (Ref. 2) has motivated many physicists to examine in detail the mechanisms at work in such magnetic and superconducting systems. In a previous paper[3] we presented a model where the superconducting electrons are the $4d$ electrons of Rh or Mo, and the rare-earth ions carry the magnetic moments which interact among them through the indirect coupling induced by the $5d$ and $6s$ electrons of rare-earth ions. The spin-dependent interaction between the superconducting electrons and the rare-earth ions is known to be relatively weak.[4] In this model, the electromagnetic interplay between the superconducting electron system and the magnetic spin system becomes important; the ferromagnetic nature of the spin system and the diamagnetic nature of the superconducting system compete through the electromagnetic interaction. The diamagnetic nature, arising from the Meissner current, tends to shield the spin magnetic moment, while the ferromagnetic nature tries to correlate the localized spins. Many phenomena can be understood in terms of these two effects and several predictions have been made; these are the presence of the spin-periodic phase,[5,6] superconducting domain wall,[7,8] self-induced vortices,[9,10] spontaneous surface magnetization and the oscillatory penetration of the magnetic field,[11] and the strong shielding of the forward neutron scattering.[12] The Meissner-type shielding of spin fluctuation can be verified by the measurement of ultrasonic attenuation.[13] Experiments of this kind have been successfully performed.[14]

As for the possible phase in the bulk system, it was pointed out that, even at $H=0$, the paramagnetic Meissner state, the ferromagnetic Meissner state, the spin-periodic Meissner state, the self-induced vortex state, and the ferro- (or para-) magnetic normal state are possible, depending on the choice of the parameters.[5,9,15] In the mixed state, there is a tendency of a type-II/2 superconductor changing to a type-II/1 (or to type-I) superconductor with decreasing temperature,[3] since the magnetic ions enhance the attractive interaction.[3,16]

In the previous paper,[3] we used an approximation in which the saturation effect of the magnetic moments is neglected. However, the latter effect becomes important at lower temperatures and can, under certain circumstances, induce spontaneous magnetization. In this paper, we take into account the saturation effect of the localized spins in the mean-field approximation and also present the more detailed formalism, used in the analyses in Refs. 5, 9, 11, and 15. Several typical phase diagrams in the H-T plane will be presented.[17]

We calculate the electromagnetic field created by vortices in the mixed state using a Maxwell-type equation. Multivortex effects are taken into account through the nonlinear intervortex interaction, the strength of which can be determined from a thermodynamical argument. Our analysis covers the entire domain of the applied field, i.e., $H_{c1} \leq H \leq H_{c2}$. If the s-f interaction is comparable with the electromagnetic interaction, one should also consider the pair-breaking effect of Cooper pairs and the spin polarization effect on the conduction electrons. Since the s-f interaction is known to be weak, we may approximately include these effects through a renormalization of the various parameters, assuming that

temperature dependence of the renormalization is mild. A detailed estimation of the correction due to s-f interaction is in progress.

The outline of the present paper is as follows: In Sec. II, starting with a microscopic Hamiltonian, we derive the Gibbs free energy of magnetic superconductors and the basic equations which determine electromagnetic properties. The approximation method used in this paper is explained. In Sec. III, a simplified approximation is introduced. Various critical fields are discussed in Sec. IV. Section V is devoted to a discussion of the numerical calculations. Section VI summarizes the main results of this paper.

II. THE FREE ENERGY AND THE BASIC EQUATIONS

In order to make the present paper self-contained, we present in this section a brief account of a derivation of the Gibbs free energy and a summary of the basic equations.

In the present paper, we use the derivative operator notation such as $F(-i\vec{\nabla})$. The operation of $F(-i\vec{\nabla})$ is defined through its Fourier transform:

$$F(-i\vec{\nabla})\exp(i\vec{k}\cdot\vec{x})=F(\vec{k})\exp(i\vec{k}\cdot\vec{x})\ . \tag{2.1}$$

When the Fourier form of a function $g(\vec{x})$ is given by

$$g(\vec{x})=\int d^3k\, e^{i\vec{k}\cdot\vec{x}}G(\vec{k})\ , \tag{2.2}$$

the $F(-i\vec{\nabla})g(\vec{x})$ and $F^{-1}(-i\vec{\nabla})g(\vec{x})$ are abbreviations for

$$F(-i\vec{\nabla})g(\vec{x})=\int d^3k\, e^{i\vec{k}\cdot\vec{x}}F(\vec{k})G(\vec{k})\ , \tag{2.3a}$$

$$F^{-1}(-i\vec{\nabla})g(\vec{x})=\int d^3k\, e^{i\vec{k}\cdot\vec{x}}F^{-1}(\vec{k})G(\vec{k})\ , \tag{2.3b}$$

respectively. We also use the notation

$$\langle\vec{x}\,|\,F(-i\vec{\nabla})\,|\,\vec{y}\rangle =\frac{1}{(2\pi)^3}\int d^3k\,F(\vec{k})\exp[i\vec{k}\cdot(\vec{x}-\vec{y})]\ , \tag{2.4}$$

which gives

$$F(-i\vec{\nabla})g(\vec{x})=\int d^3y\frac{1}{(2\pi)^3}\int d^3k\,F(\vec{k})\exp[i\vec{k}\cdot(\vec{x}-\vec{y})]g(\vec{y})=\int d^3y\langle\vec{x}\,|\,F(-i\vec{\nabla})\,|\,\vec{y}\rangle g(\vec{y})\ . \tag{2.5}$$

This shows that derivative operators act as nonlocal form factors.

Since the purpose of this paper is to consider the saturation effects of the spin system, we begin with the microscopic Hamiltonian. As will be shown later, the ground-state energy in Ref. 3 will be obtained from this microscopic Hamiltonian in the lowest-order approximation. In the present paper, this approximation is avoided.

The Hamiltonian is given by

$$\begin{aligned}H(\vec{x})=&\psi^\dagger(\vec{x})\epsilon\{-i[\vec{\nabla}+(ie/\hbar c)\vec{A}(\vec{x})]\}\psi(\vec{x})\\&-\lambda\psi_\uparrow^\dagger(\vec{x})\psi_\downarrow^\dagger(\vec{x})\psi_\downarrow(\vec{x})\psi_\uparrow(\vec{x})\\&+\frac{1}{8\pi}\vec{B}^2(\vec{x})-\vec{B}(\vec{x})\cdot\vec{M}(\vec{x})\\&-\tfrac{1}{2}\vec{M}(\vec{x})\cdot\gamma_0(-i\vec{\nabla})\vec{M}(\vec{x})\ .\end{aligned} \tag{2.6}$$

Here $\epsilon(\vec{k})$ is assumed to be parabolic, $\epsilon(\vec{k})=(\hbar^2/2m)(\vec{k}^2-\vec{k}_F^2)$, $\vec{A}(\vec{x})$ is the vector potential, $\vec{B}(\vec{x})$ $[\equiv\vec{\nabla}\times\vec{A}(\vec{x})]$ is the magnetic induction field, and $\vec{M}(\vec{x})$ is the magnetic moment given by

$$\vec{M}(\vec{x})=g\mu_B\sum_n\vec{S}_n\delta(\vec{x}-\vec{R}_n)\ , \tag{2.7}$$

with $\vec{S}_n$ being the localized spin, of magnitude J, situated at the lattice point $\vec{R}_n$. The spin-spin interaction γ_0 is mediated by exchange interactions other than the dipole interaction. (The temperature dependent of γ_0 will be neglected.)

For the purpose of computing the ground-state energy, it is convenient to separate (2.6) into two parts. The magnetic energy $W_m(\vec{x})$ is given in the Hartree approximation by

$$\begin{aligned}W_m(\vec{x})=&\frac{1}{8\pi}\vec{B}^2(\vec{x})-\vec{B}(\vec{x})\cdot\vec{M}(\vec{x})\\&-\tfrac{1}{2}\vec{M}(\vec{x})\cdot\gamma_0(-i\vec{\nabla})\vec{M}(\vec{x})\ ,\end{aligned} \tag{2.8}$$

while the electronic energy $W_e(\vec{x})$ is defined by

$$\begin{aligned}W_e(\vec{x})=&\left\langle 0\left|\psi^\dagger(\vec{x})\epsilon\left[-i\left[\vec{\nabla}+\frac{ie}{\hbar c}\vec{A}(\vec{x})\right]\right]\psi(\vec{x})\right.\right.\\&\left.\left.-\lambda\psi_\uparrow^\dagger(\vec{x})\psi_\downarrow^\dagger(\vec{x})\psi_\downarrow(\vec{x})\psi_\uparrow(\vec{x})\right|0\right\rangle\ .\end{aligned} \tag{2.9}$$

In (2.8) and (2.9), $\vec{B}(\vec{x})$, $\vec{M}(\vec{x})$, and $\vec{A}(\vec{x})$ are understood to be c-numbers in the Hartree approximation; they correspond to the vacuum expectation values $\langle 0\,|\,\vec{B}(\vec{x})\,|\,0\rangle$, $\langle 0\,|\,\vec{M}(\vec{x})\,|\,0\rangle$, and $\langle 0\,|\,\vec{A}(\vec{x})\,|\,0\rangle$,

respectively. When certain topological objects (such as vortices) are induced, the electron field carries a phase factor $\exp[if(\vec{x})]$. Such objects are stable in the superconductive state. (They are unstable in the normal state.) By extracting this phase factor from $\psi(\vec{x})$, one sees that $\vec{A}(\vec{x})$ and $f(\vec{x})$ always appear in the combination $\vec{A}_f(\vec{x})=\vec{A}(\vec{x})-(\hbar c/e)\vec{\nabla}f(\vec{x})$ in the expression for the ground-state energy. This is a result of gauge invariance. Quite generally, we can write $W_e(\vec{x})$ in (2.9) in the following manner:

$$W_e(\vec{x})=-W_0+\frac{1}{2c}\vec{J}(\vec{A}_f(\vec{x}))\cdot\vec{A}_f(\vec{x}) +E_{\text{core}}(\vec{x}) , \tag{2.10}$$

where W_0 is the condensation energy, $\vec{J}\,A(f(\vec{x}))$ is the electric current, and $E_{\text{core}}(\vec{x})$ is the remaining part of the electronic energy density. We note the following:

(i) W_0 corresponds to W_e for $\vec{A}_f(\vec{x})=0$.

(ii) The bilinear term of $\vec{A}_f(\vec{x})$ appears only through the $\vec{J}(\vec{A}_f(\vec{x}))$ term.

(iii) $E_{\text{core}}(\vec{x})$ contains only terms higher than second order in $\vec{A}_f(\vec{x})$.

The term in linear $\vec{A}_f$ in the current $\vec{J}(\vec{A}_f(\vec{x}))$, which we denote by $\vec{j}(\vec{A}_f(\vec{x}))$, has the form

$$\frac{4\pi}{c}\vec{j}(\vec{A}_f(\vec{x}))=-\lambda_L^{-2}(t)C(-i\vec{\nabla})\vec{A}_f(\vec{x}) , \tag{2.11}$$

where λ_L is the London penetration depth and $C(-i\vec{\nabla})$ is a nonlocal kernel which is obtained from the photon self-energy; t is the reduced temperature T/T_c, with T_c denoting the superconducting transition temperature. When $C(\vec{k})$ is calculated in the one-loop approximation, it reduces to the well-known BCS kernel, while the multiloop contribution, evaluated in Refs. 18–20, includes a contribution from the collective mode and leads to a generalized Pippard-type kernel referred to as the c function.

We see, from (2.6), that the mean field experienced by the magnetic moments is given by

$$\vec{H}_m(\vec{x})=\vec{B}(\vec{x})+\gamma_0(-i\vec{\nabla})\vec{M}(\vec{x}) . \tag{2.12}$$

The entropy $S(\vec{x})$ of the system in the mean-field approximation is thus given by

$$TS(\vec{x})=TS_e+k_BTN\ln Z_J((g\mu_BJ/k_BT)\,|\,\vec{H}_m(\vec{x})\,|\,) -\vec{H}_m(\vec{x})\cdot\vec{M}(\vec{x}) , \tag{2.13}$$

where S_e is the entropy of the electrons and

$$Z_J(y)=\sinh\left[\frac{2J+1}{2J}y\right]\Big/\sin\left[\frac{1}{2J}y\right] . \tag{2.14}$$

Here J is the spin of rare-earth ions. The fields $\vec{B}(\vec{x})$ and $\vec{M}(\vec{x})$ satisfy the following equations:

$$\vec{\nabla}\times\vec{B}(\vec{x})=\frac{4\pi}{c}\vec{J}(\vec{A}_f(\vec{x}))+4\pi\vec{\nabla}\times\vec{M}(\vec{x}) , \tag{2.15}$$

$$|\,\vec{M}(\vec{x})\,|=g\mu_BJB_J((g\mu_BJ/k_BT)\,|\,\vec{H}_m(\vec{x})\,|\,) , \quad \vec{M}(\vec{x})\|\vec{H}_m(\vec{x}) . \tag{2.16}$$

Equation (2.15) is the Maxwell equation. The electric current $\vec{J}(\vec{A}_f)$ is given by (2.11) in the linear approximation. In Eq. (2.16), B_J is the Brillouin function. In the derivation of Eq. (2.16) use was made of the mean-field approximation. The magnetization $\vec{M}(\vec{x})$ and the mean field $\vec{H}_m(\vec{x})$ should be parallel to each other.

When the vortex lattice structure is specified and the vortex density n is given, the free-energy density becomes a function of n:

$$F_s(n)=\frac{1}{V}\int_V d^3x[W_m(\vec{x})+W_e(\vec{x})-TS(\vec{x})] . \tag{2.17}$$

Since

$$W_m(\vec{x})-T[S(\vec{x})-S_e] =\frac{1}{8\pi}\vec{B}(\vec{x})\cdot\vec{H}(\vec{x})+\tfrac{1}{2}\vec{M}(\vec{x})\cdot\vec{B}(\vec{x}) -\int^{\vec{B}(\vec{x})}d\vec{B}'(\vec{x})\cdot\vec{M}'(\vec{x}) ,$$

with $\vec{M}'(\vec{x})$ related to $\vec{B}'(\vec{x})$ through (2.12) and (2.16), a linear approximation for $\vec{B}'(\vec{x})$ and $\vec{M}'(\vec{x})$ leads to the result

$$W_m(\vec{x})-T[S(x)-S_e]\simeq\frac{1}{8\pi}\vec{B}(\vec{x})\cdot\vec{H}(\vec{x}) ,$$

which was used in the calculation of the magnetostatic energy in Ref. 3. When we eliminate $\vec{J}(\vec{A}_f(\vec{x}))$ from $W_e(\vec{x})$ [cf. (2.10)] by means of the Maxwell equation (2.15), $F_s(n)$ in (2.17) is rewritten as

$$F_s(n)=\frac{1}{V}\int_V d^3x\left[\frac{1}{8\pi}\vec{n}(\vec{x})\phi\cdot\vec{H}(\vec{x})+\tfrac{1}{2}\vec{H}_m(\vec{x})\cdot\vec{M}(\vec{x})-k_BTN\ln Z_J((g\mu_BJ/k_BT)\,|\,\vec{H}_m(\vec{x})\,|\,) -\frac{H_c^2}{8\pi}+E_{\text{core}}(\vec{x})\right] , \tag{2.18}$$

where we have used integration by parts. The second and third terms in (2.18) arise from the nonlinearity of spins and exhibit saturation effects. Those terms become important especially when spontaneous magnetization is induced. The quantity $\vec{n}(\vec{x})\phi$ is given by

$$\vec{n}(\vec{x})\phi=\frac{\hbar c}{e}\vec{\nabla}\times\vec{\nabla}f(\vec{x}) , \tag{2.19}$$

with ϕ being the unit flux $hc/2e$, $\vec{H}(\vec{x})$ is a local magnetic field defined by

$$\vec{H}(\vec{x})=\vec{B}(\vec{x})-4\pi\vec{M}(\vec{x}) , \tag{2.20}$$

and $H_c^2/8\pi$ ($\equiv W_0+TS_e$) is the condensation energy obtained from the BCS theory. (Note that the s-f interaction is neglected.) When a vortex is situated at the origin along the third axis, $f(\vec{x})$ is given by

$$f(\vec{x})=\tan^{-1}(x_2/x_1) , \tag{2.21}$$

which leads to

$$\frac{\hbar c}{e}\vec{\nabla}\times\vec{\nabla}f(\vec{x})=\phi\vec{e}_3\delta(x_1)\delta(x_2) . \tag{2.22}$$

The relation $\vec{\nabla}\times\vec{\nabla}f(\vec{x})\neq 0$ manifests the topologically singular nature of the vortex. When the vortices form a lattice and their positions are denoted by $\vec{\zeta}_i=(\zeta_{i1},\zeta_{i2},0)$, $\vec{n}(\vec{x})$ is given by

$$\vec{n}(\vec{x})=\sum_i \vec{e}_3\delta^{(2)}(\vec{x}-\vec{\zeta}_i) . \tag{2.23}$$

When the current $\vec{J}(\vec{A}_f(\vec{x}))$ in the Maxwell equation is approximated by the linear current $\vec{j}(\vec{A}_f(\vec{x}))$, $\vec{B}(\vec{x})$ is obtained from (2.11) and (2.15) as

$$\vec{B}(\vec{x})=\frac{\lambda_L^{-2}C(-i\vec{\nabla})}{-\nabla^2+\lambda_L^{-2}C(-i\vec{\nabla})}\vec{n}(\vec{x})\phi - \frac{4\pi\nabla^2}{-\nabla^2+\lambda_L^{-2}C(-i\vec{\nabla})}[\mathcal{T}]\vec{M}(\vec{x}) , \tag{2.24}$$

where $[\mathcal{T}]$ is the transverse projection operator and is given by

$$[\mathcal{T}]_{ij}=\delta_{ij}-(\nabla_i\nabla_j/\nabla^2) . \tag{2.25}$$

Note that $\vec{n}(\vec{x})\phi$ is transverse. Then $\vec{H}(\vec{x})$ and $\vec{H}_m(\vec{x})$ are given by

$$[\mathcal{T}]\vec{H}(\vec{x})=\frac{\lambda_L^{-2}C(-i\vec{\nabla})}{-\nabla^2+\lambda_L^{-2}C(-i\vec{\nabla})}\vec{n}(\vec{x})\phi - 4\pi\frac{\lambda_L^{-2}C(-i\vec{\nabla})}{-\nabla^2+\lambda_L^{-2}C(-i\vec{\nabla})}[\mathcal{T}]\vec{M}(\vec{x}) , \tag{2.26}$$

$$H_m(\vec{x})=\frac{\lambda_L^{-2}C(-i\vec{\nabla})}{-\nabla^2+\lambda_L^{-2}C(-i\vec{\nabla})}\vec{n}(\vec{x})\phi + \tilde{\gamma}(-i\vec{\nabla})\vec{M}(\vec{x}) , \tag{2.27}$$

with

$$\tilde{\gamma}(-i\vec{\nabla})=\gamma(-i\vec{\nabla}) - 4\pi\frac{\lambda_L^{-2}C(-i\vec{\nabla})}{-\nabla^2+\lambda_L^{-2}C(-i\vec{\nabla})}[\mathcal{T}] , \tag{2.28}$$

$$\gamma(-i\vec{\nabla})=\gamma_0(-i\vec{\nabla})+4\pi[\mathcal{T}] . \tag{2.29}$$

Here we made use of Eq. (2.12).

The exchange interaction in the normal state, which we denote by $\gamma(\vec{k})$ [see (2.41)], is usually parametrized as

$$[\mathcal{T}]_{ij}\gamma_{jl}(\vec{k})=\left[\frac{T_m}{\Theta_C}-\frac{D}{\Theta_C}\vec{k}^2\right][\mathcal{T}]_{il} , \tag{2.30}$$

where Θ_C is the Curie constant given by $(g\mu_B)^2J(J+1)/3k_B$. Since $\gamma(\vec{k})$ and the staggered susceptibility $\chi(\vec{k})$ of the normal state are related through

$$\chi(\vec{k})=\frac{\Theta_C}{T-\Theta_c\gamma(\vec{k})}=\frac{\Theta_C}{T-T_m+D\vec{k}^2} ,$$

then T_m is the Curie temperature of the normal state and D the stiffness constant. When (2.26) and (2.27) are considered, (2.18) gives

$$F_s(n)=\frac{1}{V}\int_V d^3x\left[\frac{1}{8\pi}\vec{n}(\vec{x})\phi\cdot\frac{\lambda_L^{-2}C(-i\vec{\nabla})}{-\nabla^2+\lambda_L^{-2}C(-i\vec{\nabla})}\vec{n}(\vec{x})\phi-\frac{H_c^2}{8\pi}+E_{\text{core}}(\vec{x})+\tfrac{1}{2}\vec{M}(\vec{x})\cdot\tilde{\gamma}(-i\vec{\nabla})\vec{M}(\vec{x}) - k_BTN\ln Z_J((g\mu_BJ/k_BT)\,|\,\vec{H}_m(\vec{x})\,|\,)\right] . \tag{2.31}$$

The free-energy expressions of Eqs. (2.18) and (2.31) imply the following two interpretations of the mechanisms at work in the magnetic superconductors. On the one hand, Eq. (2.18) shows that the vortex interaction is given by the magnetic field $\vec{H}(\vec{x})$ and that the induced magnetization further

reduces the free energy of the system. The latter effect permits in certain cases the formation of a self-induced vortex state. On the other hand, Eq. (2.31) shows that the spin-spin interaction is modified to $\tilde{\gamma}(-i\vec{\nabla})$ by the shielding effect of the spin fluctuations due to the Meissner current. An important difference of this system from the fictitious homogeneous system with spin interaction $\tilde{\gamma}(-i\vec{\nabla})$ is that the field

$$\vec{b}_0(\vec{x})=\frac{\lambda_L^{-2}C(-i\vec{\nabla})}{-\nabla^2+\lambda_L^{-2}C(-i\vec{\nabla})}\vec{n}(\vec{x})\phi \tag{2.32}$$

is no longer spatially invariant.

To calculate $\vec{H}(\vec{x})$ and $E_{\text{core}}(\vec{x})$ in (2.18) including all of the nonlinear effects of $\vec{A}_f(\vec{x})$ is quite a difficult task. In order, therefore, to calculate the n dependence (n is the vortex density) of the free energy from $n=0$ to $n=n_c$ (at H_{c2}), a certain simple approximation method is needed. Our approximation method is formulated as follows: Suppose that we know $\vec{B}(\vec{x})$ and $E_{\text{core}}(\vec{x})$ for a single vortex which we denote $\vec{b}_s(\vec{x})$ and $\epsilon^s_{\text{core}}(\vec{x})$, respectively. Owing to the flux quantization, $\vec{b}_s(\vec{x})$ is a well-localized function. Therefore, when the vortices form a lattice, we can approximate $\vec{B}(\vec{x})$ by

$$\vec{B}(\vec{x})=\sum_i \vec{b}_s(\vec{x}-\vec{\xi}_i)\ . \tag{2.33}$$

The contribution from $E_{\text{core}}(\vec{x})$ to the free-energy density is given by the integration in a unit cell of the vortex lattice

$$nE_{\text{core}}(n)=\frac{1}{\Omega}\int_\Omega d^3x\, E_{\text{core}}(\vec{x})\ . \tag{2.34}$$

Here it was considered that $1/\Omega$ is the vortex density n. In the limit $\Omega\to\infty$, the result is the core energy of a single vortex:

$$E_{\text{core}}(0)=\int d^3x\,\epsilon^s_{\text{core}}(\vec{x})=E_1\ . \tag{2.35}$$

When $\Omega\neq\infty$, since $E_{\text{core}}(\vec{x})$ is a functional of $\vec{B}(\vec{x})$, we can expand $E_{\text{core}}(\vec{x})$ in powers of $\vec{b}_{\text{in}}(\vec{x})$ defined by

$$\vec{b}_{\text{in}}(\vec{x})=\sum_{i\neq 0}\vec{b}_s(\vec{x}-\vec{\xi}_i)\ , \tag{2.36}$$

which is the magnetic induction due to the vortices outside the cell Ω:

$$E_{\text{core}}(\vec{x})=\epsilon^s_{\text{core}}(\vec{x})+\int d^3y\frac{\delta E_{\text{core}}(\vec{x})}{\delta\vec{B}(\vec{y})}\vec{b}_{\text{in}}(\vec{y})+\cdots\ . \tag{2.37}$$

Since $\vec{b}_s(\vec{x})$ is a well-localized function [i.e., $\vec{b}_s(\vec{x})$ is very small for $|\vec{x}|>\xi$], $\epsilon^s_{\text{core}}(\vec{x})$ is also well localized. Therefore, $\delta\epsilon^s_{\text{core}}(\vec{x})/\delta\vec{b}_s(\vec{y})$ can be roughly approximated by a δ function. Performing the spatial integration of $E_{\text{core}}(\vec{x})$, using the above approximations, we see that $E_{\text{core}}(n)$ has the following expansion

$$E_{\text{core}}(n)=E_1-E_2\sum_{i\neq 0}b_s(\vec{\xi}_i)+\cdots\ . \tag{2.38}$$

Thus we see that the E_2 term represents the nonlinear effect of multiple vortices. When the vortex-lattice length is larger than ξ, we may ignore the higher-order terms represented by the ellipses in (2.38). We determine E_2 by the requirement that the phase transition at H_{c2} is second order. In this way the evaluation of the free energy is reduced to the calculation of E_1 and $\vec{b}_s(\vec{x})$. [In Ref. 3, $h_s(\vec{\xi}_i)$, the magnetic field, is used instead of $b_s(\vec{\xi}_i)$ in the evaluation of the core energy. The above argument shows that (2.38) is more appropriate, since $\vec{b}_s(\vec{x})$ damps exponentially while $\vec{h}_s(\vec{x})$ does not.]

The argument until now holds true for any approximation method, provided $\vec{b}_s(\vec{x})$ is well localized with the well-known asymptotic form $K_0(r/\lambda_L)$ for $|\vec{x}|\gg\xi$. Therefore, the detailed quantitative differences between various approximation methods [such as the Gor'kov equation with the random-phase approximation (RPA), the boson method, etc.] originate from the behavior of $\vec{b}_s(\vec{x})$ (and therefore, of the single-vortex current) at $|\vec{x}|\lesssim\xi$. The linear single-vortex current $\vec{j}$ given by the boson method shows a reasonable behavior in the sense that (a) it vanishes at the vortex center and (b) it increases smoothly with increasing $|\vec{x}|$ until it reaches a maximum at $|\vec{x}|\simeq\xi$, reflecting the effect of the collective mode. Therefore, we expect that the $\vec{b}_s$ used in the boson method should lead to reasonable results in the evaluation of the free energy. The linear single-vortex current given by the Gor'kov equation, with RPA, diverges at the center because its kernel $C(\vec{k})$ is the BCS kernel, which is calculated only to one-loop approximation, and therefore does not take into account the effect of the collective mode. This indicates that the nonlinear effect is of vital significance. When the nonlinear terms of $\vec{A}_f$ are considered, the behavior of $\vec{J}$ for the single vortex becomes rather similar to that of the linear current $\vec{j}$ of the boson method (though the increase of $\vec{J}$ at $|\vec{x}|<\xi$ at $T\simeq 0$ is much steeper than that of the current $\vec{j}$ calculated in the boson method). Therefore, we expect that the $\vec{b}_s$ used in the boson method and that of the Gor'kov equation with RPA should lead to qualitatively similar results in the evaluation of the free energy.

Admittedly the evaluation of E_1 has been crude and semiphenomenological.[19] However, since it has led to a reasonable qualitative—frequently, quant-

itative—agreement between theoretical results and experiments for nonmagnetic superconductors,[21,22] we use the same E_1 in the present study of magnetic superconductors.

In summary, the free energy is given by (2.18) and the basic equations are (2.15) with (2.11) and (2.16) with (2.12). The nonlinear effect of the vector potential in the electronic energy $E_{\text{core}}(\vec{x})$ is evaluated by (2.38).

We now derive the free energy in the normal state. In the normal state, the internal magnetic field is equal to the external magnetic field:

$$\vec{H}(\vec{x})=\vec{H} . \tag{2.39}$$

Therefore, the magnetization satisfies the usual self-consistent equation

$$|\vec{M}_H|=g\mu_B JB_J[(g\mu_B J/k_B T)|\vec{H}_m|] \tag{2.40}$$

with

$$\vec{H}_m=\vec{H}+\gamma(-i\vec{\nabla})\vec{M}_H , \tag{2.41}$$

where $\vec{B}=\vec{H}+4\pi\vec{M}_H$ is used and $\gamma(-i\vec{\nabla})$ is given by (2.30). The free energy of the normal state is obtained from (2.17) by putting $\vec{J}(\vec{x})=\vec{0}$, $H_c^2/8\pi=0$, $E_{\text{core}}(\vec{x})=0$, and $\vec{B}=\vec{H}+4\pi\vec{M}_H$. The result is

$$F_n(\vec{H})=-\frac{\vec{H}^2}{8\pi}+F_m(\gamma,\vec{H})+\frac{1}{4\pi}\vec{H}\cdot\vec{B} , \tag{2.42}$$

where

$$F_m(\gamma,\vec{H})=\tfrac{1}{2}\gamma(\vec{0})\vec{M}_H^2 - k_B TN\ln Z_J \times[(g\mu_B J/k_B T)|\vec{H}+\gamma(\vec{0})\vec{M}_H|] , \tag{2.43}$$

We have

$$\gamma(\vec{0})=T_m/\Theta_C . \tag{2.44}$$

In this paper we neglected the weak s-f interaction (or assumed that the s-f interaction could be approximately included through a temperature-independent renormalization). When the s-f interaction is considered, $H_c^2/8\pi$, the c function, and $\gamma_0(-i\vec{\nabla})$ should be modified accordingly. A study in this direction is now in progress.

III. THE APPROXIMATION

In solving the basic equations (2.15) and (2.16) presented in Sec. II, we separate each field into its spatially averaged value and its deviation as

$$\vec{B}(\vec{x})=n\phi\vec{e}_3+\vec{b}(\vec{x}) , \tag{3.1a}$$

$$\vec{M}(\vec{x})=\vec{m}_0+\vec{m}(\vec{x}) , \tag{3.1b}$$

$$\vec{H}(\vec{x})=\vec{h}_0+\vec{h}(\vec{x}) . \tag{3.1c}$$

Here n is vortex density. We now make use of the linear approximation and consider only the lowest-order effects of the deviations. In the following, we assume that all fields are along the third axis, so that we omit the arrows which indicate vectors. We require that the average values satisfy (2.16):

$$m_0=g\mu_B JNB_J\{(g\mu_B J/k_B T)[n\phi+\tilde{\gamma}(\vec{0})m_0]\} . \tag{3.2}$$

In this sense, the nonlinear effect (and therefore the saturation effect) is considered only for the averaged values $n\phi$, m_0, and h_0. When we consider only the linear terms in m, h, and b, (2.16) leads to

$$m(\vec{x})=\chi(-i\vec{\nabla})h(\vec{x}) \tag{3.3a}$$

$$=\frac{\chi(-i\vec{\nabla})}{1+4\pi\chi(-i\vec{\nabla})}b(\vec{x}) , \tag{3.3b}$$

where

$$\chi(-i\vec{\nabla})=\frac{\alpha_J\Theta_C}{T-\alpha_J T_m-\alpha_J D\nabla^2} , \tag{3.4}$$

$$\alpha_J=[3J/(J+1)]B_J' \times\{(g\mu_B J/k_B T)[n\phi+\tilde{\gamma}(0)m_0]\} . \tag{3.5}$$

When (2.15) with (2.11) and (3.3b) are used, we obtain

$$b(\vec{x})=\frac{[1+4\pi\chi(-i\vec{\nabla})]\lambda_L^{-2}C(-i\vec{\nabla})}{-\nabla^2+[1+4\pi\chi(-i\vec{\nabla})]\lambda_L^{-2}C(-i\vec{\nabla})} \times[n(\vec{x})\phi-n\phi] , \tag{3.6}$$

and

$$h(\vec{x})=\frac{\lambda_L^{-2}C(-i\vec{\nabla})}{-\nabla^2+[1+4\pi\chi(-i\vec{\nabla})]\lambda_L^{-2}C(-i\vec{\nabla})} \times[n(\vec{x})\phi-n\phi] . \tag{3.7}$$

When we define the effective single-vortex field by

$$h_s(\vec{x})=\frac{\phi}{(2\pi)^2}\int d^2k\, e^{i\vec{k}\cdot\vec{x}} \times\frac{\lambda_L^{-2}C(\vec{k})}{\vec{k}^2+[1+4\pi\chi(\vec{k})]\lambda_L^{-2}C(\vec{k})} , \tag{3.8a}$$

$$b_s(\vec{x})=\frac{\phi}{(2\pi)^2}\int d^2k\, e^{i\vec{k}\cdot\vec{x}} \times\frac{[1+4\pi\chi(\vec{k})]\lambda_L^{-2}C(\vec{k})}{\vec{k}^2+[1+4\pi\chi(\vec{k})]\lambda_L^{-2}C(\vec{k})}\,, \tag{3.8b}$$

(2.23) gives

$$h(\vec{x})=\frac{-n\phi}{1+4\pi\chi(0)}+\sum_i h_s(\vec{x}-\vec{\xi}_i)\,, \tag{3.9a}$$

$$b(\vec{x})=\sum_i b_s(\vec{x}-\vec{\xi}_i)-n\phi\,. \tag{3.9b}$$

With our approximation, the free energy (2.18) can be calculated up to the second order in b, h, and m. The contributions of b, h, and m to the second term on the right-hand side of (2.18) compensate those to the third term. Calculation of the first term in (2.18) yields

$$\begin{aligned}\frac{1}{V}\int d^3x\frac{1}{8\pi}n(\vec{x})\phi\cdot H(\vec{x})&=\frac{1}{V}\int d^3x\frac{\phi}{8\pi}\sum_i\delta^{(2)}(\vec{x}-\vec{\xi}_i)H(\vec{x})\\&=\frac{n\phi}{8\pi}H(\vec{x}=\vec{0})\\&=\frac{n\phi}{8\pi}[n\phi-4\pi m_0+h(\vec{0})]\,,\end{aligned}$$

where we have chosen one of the lattice points as the origin of the coordinate system and used the periodicity of the spin lattice. Note that $\tilde{\gamma}(\vec{0})=\gamma_0(\vec{0})$ according to (2.28) and (2.29). Then the free-energy density is obtained as follows:

$$F_s(n)=\frac{n\phi}{8\pi}[n\phi+h(\vec{0})]+F_m(\tilde{\gamma},n) -\frac{H_c^2}{8\pi}+nE_{\rm core}(n)\,, \tag{3.10}$$

where

$$\begin{aligned}F_m(\tilde{\gamma},n)=&\tfrac{1}{2}\tilde{\gamma}(\vec{0})m_0^2\\&-k_BTN\ln Z_J\\&\times\{(g\mu_BJ/k_BT)[n\phi+\tilde{\gamma}(\vec{0})m_0]\}\end{aligned} \tag{3.11}$$

and $E_{\rm core}(n)$ is the core energy defined in (2.34). According to (2.38), we have

$$E_{\rm core}(n)=E_1-E_2b^{\rm int}(n)\,. \tag{3.12}$$

Here[19]

$$E_1=\frac{\hbar^2c^2}{32e^2\lambda_L^2}=\frac{\phi}{\lambda_L^2}\frac{\phi}{8\pi}\frac{1}{4\pi}\,, \tag{3.13}$$

$$b^{\rm int}(n)=\sum_{i\neq0}b_s(\vec{\xi}_i)\,, \tag{3.14}$$

and, as discussed in Sec. II, E_2 is determined thermodynamically. Finally, we have

$$F_s(n)=\frac{n\phi}{8\pi}g(n)+F_m(\tilde{\gamma},n)-\frac{H_c^2}{8\pi}\,, \tag{3.15}$$

$$g(n)=n\phi+h(\vec{0})+\epsilon_1-\epsilon_2b^{\rm int}(n)\,, \tag{3.16}$$

$$\epsilon_1=\frac{E_1}{\phi/8\pi}=\frac{\phi}{\lambda_L^2}\frac{1}{4\pi},\quad \epsilon_2=\frac{E_2}{\phi/8\pi}\,. \tag{3.17}$$

When the vortices form a lattice, the lattice sum in $h(\vec{0})$ and $b^{\rm int}(n)$ can be rewritten in terms of the sum over the reciprocal lattice:

$$h(\vec{0})=n\phi\sum_{\vec{K}\neq0}\frac{\lambda_L^{-2}C(\vec{K})}{K^2+[1+4\pi\chi(\vec{K})]\lambda_L^{-2}C(\vec{K})}\,, \tag{3.18}$$

$$b^{\rm int}(n)=n\phi\left[1+\sum_{\vec{K}\neq0}\frac{[1+4\pi\chi(\vec{K})]\lambda_L^{-2}C(\vec{K})}{\vec{K}^2+[1+4\pi\chi(\vec{K})]\lambda_L^{-2}C(\vec{K})}\right]-b_s(\vec{0}) \tag{3.19}$$

The approximation used in this section will be referred to as the linear approximation.

IV. CRITICAL FIELDS

The Gibbs free energy of the mixed state with an applied field H is a function of vortex density n and is given by

$$G_s(n)=\frac{n\phi}{8\pi}g(n)+F_m(\tilde{\gamma},n\phi)-\frac{H_c^2}{8\pi}-\frac{n\phi}{4\pi}H\,. \tag{4.1}$$

In particular, $n=0$ leads to the free energy of the Meissner state. Note that the Meissner state is not necessarily homogeneous, since the periodic phase

which maximizes $\tilde{\gamma}(\vec{k})$ with respect to $\vec{k}$ (and therefore minimizes the free energy) is possible as was pointed out in Refs. 5 and 6. In the isotropic case, this periodic phase is the spin-spiral phase. A strong anisotropy may change this to the spin-sinusoidal phase. When the spin-spiral phase in the Meissner state ($n=0$) appears, $\tilde{\gamma}(\vec{0})$ and m_0 in (3.11) should be replaced by $\tilde{\gamma}(\vec{P})$ and m_P, where $\vec{P}$ is the value of $\vec{k}$ which maximizes $\tilde{\gamma}(\vec{k})$. Then, the free energy is

$$G_M = F_m(\tilde{\gamma}(\vec{P}),0) - H_c^2/8\pi \ , \tag{4.2}$$

with

$$F_m(\tilde{\gamma}(\vec{P}),0) = \tfrac{1}{2}\tilde{\gamma}(\vec{P})m_P^2 - k_B T N \ln Z_J \times[(g\mu_B J/k_B T)\tilde{\gamma}(\vec{P})m_P] \ , \tag{4.3}$$

$$\tilde{\gamma}(\vec{P}) = \max_{\vec{k}} \tilde{\gamma}(\vec{k}) \ , \tag{4.4}$$

$$m_P = g\mu_B JNB_J[(g\mu_B J/k_B T)\tilde{\gamma}(\vec{P})m_P] \ . \tag{4.5}$$

This state appears below the critical temperature T_P given by

$$T_P = \Theta_C \tilde{\gamma}(\vec{P}) = T_m\left[1 - \frac{D\vec{P}^2}{T_m} - \frac{4\pi\Theta_C}{T_m}\frac{\lambda_L^{-2}C(\vec{P})}{\vec{P}^2+\lambda_L^{-2}C(\vec{P})}\right] . \tag{4.6}$$

Below T_P, there is the possibility that the spiral alignment of the spins may be intertwined with the vortex flux in the mixed state for certain values of H. However, this possibility is not considered in this paper. G_M in (4.2) with $\vec{P}=0$ is the free energy of the homogeneous Meissner state.

The Gibbs free energy of the normal state is obtained by use of (2.42) as

$$G_n = -\frac{H^2}{8\pi} + F_m(\gamma,H) \tag{4.7}$$

with

$$F_m(\gamma,H) = \tfrac{1}{2}\gamma(\vec{0})m_H^2 - k_B T N \ln Z_J \times\{(g\mu_B J/k_B T)[H+\gamma(\vec{0})m_H]\} \ , \tag{4.8}$$

$$m_H = g\mu_B JNB_J\{(g\mu_B J/k_B T)[H+\gamma(\vec{0})m_H]\} \ . \tag{4.9}$$

The relation between H and n is obtained by minimizing $G_s(n)$ with respect to n: $\partial G_s(n)/\partial n = 0$. The result is

$$H(n) = \tfrac{1}{2}\left[1 + n\frac{\partial}{\partial n}\right]g(n) - 4\pi m(\tilde{\gamma},n) \ , \tag{4.10}$$

$$m(\tilde{\gamma},n) = g\mu_B JNB_J \times\{(g\mu_B J/k_B T)\times[n\phi + \tilde{\gamma}(\vec{0})m(\tilde{\gamma},n)]\} \ . \tag{4.11}$$

Note that $\gamma(\vec{0})$ and $\tilde{\gamma}(\vec{0})$ are related to each other through

$$\gamma(\vec{0}) = \tilde{\gamma}(\vec{0}) + 4\pi \ . \tag{4.12}$$

The magnetization is obtained as a function of H from (4.10) and

$$4\pi M(n) = n\phi - H(n) \ . \tag{4.13}$$

A. Upper critical field H_{c2} and ϵ_2

We require that, at the upper critical field H_{c2}, the phase transition is of second order. This leads to the conditions

$$G_s(n_c) = G_n(H_{c2}) \ , \tag{4.14}$$

$$\left.\frac{\partial G_s}{\partial H}\right|_{n_c} = \left.\frac{\partial G_n}{\partial H}\right|_{H_{c2}} , \tag{4.15}$$

or

$$n_c\phi = H_{c2} + 4\pi m_{H_{c2}} \ ,$$

where n_c is the critical flux density, i.e., the flux density at H_{c2}. From (4.12) and (4.11), one can see that

$$m(\tilde{\gamma},n_c\phi) = m_{H_{c2}} \ . \tag{4.16}$$

Thus the two conditions (4.14) and (4.15) can be written as

$$H_{c2} = n_c\phi[g(n_c) - n_c\phi] \ , \tag{4.17}$$

$$n_c\phi = \tfrac{1}{2}\left[1 + n_c\frac{\partial}{\partial n_c}\right]g(n_c) \ , \tag{4.18}$$

which determines n_c and ϵ_2 simultaneously. The upper critical field is determined by

$$H_{c2} = n_c\phi - 4\pi m(\tilde{\gamma},n_c\phi) \ . \tag{4.19}$$

B. The critical field H_c^*

The critical field H_c^* which is the boundary between the Meissner state and the normal state is ob-

tained from

$$G_n(H_c^*)=G_M \ . \tag{4.20}$$

Note that H_c^* is different, from H_c which is defined by the condensation energy (condensation energy is equal to $H_c^2/8\pi$). From (4.2) and (4.7), we have that

$$\frac{H_c^2}{8\pi}=\frac{H_c^{*2}}{8\pi}-F_m(\gamma,H_c^*)+F_m(\tilde{\gamma}(\vec{\mathrm{P}}),0) \ . \tag{4.21}$$

Since $F_m(\gamma,H_c^*)<0$ and $F_m(\tilde{\gamma}(\vec{\mathrm{P}}),0)=0$ for $T>T_P$, H_c^* is always less than H_c, since the magnetic effect reduces the critical field.

At temperature T_M which satisfies

$$\frac{H_c^2}{8\pi}=F_m(\tilde{\gamma}(\vec{\mathrm{P}}),0)-F_m(\gamma,0) \ , \tag{4.22}$$

we have that $H_c^*=0$. Since $F_m(\gamma,0)$ must be negative, this happens below T_m (the Curie temperature of the ferromagnetic phase),

$$T_M<T_m \ . \tag{4.23}$$

At this temperature, the spiral Meissner state (in the case $T_P>T_M$) or the paramagnetic Meissner state (in the case of $T_P<T_M$) makes the phase transition into the ferromagnetic normal state; T_M is the reentrant temperature. Note that, when the phase transition at H_c^* takes place, the system behaves as a type-I superconductor and the phase transition is first order.

When $T_M=0$, (4.22) leads to

$$\frac{H_c^2}{8\pi}=\frac{M^2T_m}{2\Theta_C}(1-J_P) \ ,$$

where M is the saturation value of the magnetization ($M=g\mu_B JN$) and J_P is defined by $J_P=\tilde{\gamma}(\vec{\mathrm{P}})/\gamma(\vec{0})=\tilde{\gamma}(\vec{\mathrm{P}})/(T_m\Theta_C)$. Eqs. (2.28) and (2.30) give

$$J_P=1-\frac{D\vec{\mathrm{P}}^2}{T_m}-\frac{4\pi\Theta_C}{T_m}\frac{\lambda_L^{-2}C(\vec{\mathrm{P}})}{\vec{\mathrm{P}}^2+\lambda_L^{-2}C(\vec{\mathrm{P}})} \ . \tag{4.24}$$

In order that a positive T_M exist, the following condition must be satisifed:

$$\frac{H_c^2}{8\pi}<\frac{M^2T_m}{2\Theta_C}(1-J_P) \ . \tag{4.25}$$

When the magnetic anisotropy energy is large as in $ErRh_4B_4$ and $HoMo_6S_6$, the magnetic ordering favors the sinusoidal rather than the spiral ordering. In this case, Eq. (4.21) is replaced approximately by

$$\frac{H_c^2}{8\pi}=\frac{H_c^{*2}}{8\pi}-F_m(\gamma,H_c^*)+\tfrac{1}{2}F_m(\tilde{\gamma}(\vec{\mathrm{P}}),0) \ . \tag{4.26}$$

C. Lower critical field $H(n=0)$ and H_{c1}

The magnetic field $H(n=0)$ at which a single vortex appears is obtained from (4.10) by taking the limit $n\to 0$:

$$H(0)=\tfrac{1}{2}g(0)-4\pi m(\tilde{\gamma},0) \ . \tag{4.27}$$

When $T>T_P$ [and therefore, $m(\tilde{\gamma},0)=0$], $g(0)$ is given by $h(0)+\epsilon_1$ [see (3.16)]. Then we have

$$H(0)=\tfrac{1}{2}\left[\frac{\phi}{2\pi}\int_0^\infty k\,dk\frac{\lambda_L^{-2}C(\vec{\mathrm{k}})}{\vec{\mathrm{k}}^2+[1+4\pi\chi_0(\vec{\mathrm{k}})]\lambda_L^{-2}C(\vec{\mathrm{k}})}+\epsilon_1\right] , \tag{4.28}$$

where $\chi_0(\vec{\mathrm{k}})$ denotes $\chi(\vec{\mathrm{k}})$ for $n=0$

$$\chi_0(\vec{\mathrm{k}})=\frac{\Theta_C}{T-T_m+D\vec{\mathrm{k}}^2} \ . \tag{4.29}$$

Because of our approximation, $H(0)$ here is the same as the one in Ref. 8, implying that no saturation effect is considered. When the temperature comes close to T_P, the expression (4.28), which is obtained using the linear approximation, is no longer reliable due to the appearance of the spiral phase (this is manifested by the appearance of zero point in the denominator of the integrand).

In order to go beyond the linear approximation in the calculation of $H(0)$, we return to the expression (2.31). When the integrand in (2.31) is denoted by $F(\vec{\mathrm{x}};n)$, the Gibbs free energy becomes

$$G_s(n)=\frac{n\phi}{8\pi}g_M(n)+G_s(0)-\frac{n\phi}{4\pi}H \ , \tag{4.30}$$

where

$$\frac{\phi}{8\pi}g_M(n)=\int_\Omega d^2x[F(\vec{\mathrm{x}};n)-F(\vec{\mathrm{x}};0)] \tag{4.31}$$

and Ω is the unit cell of the vortex lattice (note that $n=1/\Omega$). Then a calculation similar to the determination of (4.10) leads to

$$H(n)=\tfrac{1}{2}\left[1+n\frac{\partial}{\partial n}\right]g_M(n) \ , \tag{4.32}$$

which gives

$$H(0)=\tfrac{1}{2}g_M(0) \ . \tag{4.33}$$

Note that $g_M(0)$ is the free energy of single vortex:

$$\frac{\phi}{8\pi}g_M(0)=\int d^2x\left[\frac{\phi}{8\pi}\delta^{(2)}(\vec{x})b_0(\vec{x})+E_{\rm core}(\vec{x})+\frac{1}{2}\vec{M}(\vec{x})\tilde{\gamma}(-i\vec{\nabla})\vec{M}(\vec{x})\right.$$
$$\left.-k_BTN\ln Z_J\{(g\mu_BJ/k_BT)\,|\,\vec{H}_m(\vec{x})\,|\,\}-F_m(\tilde{\gamma},0)\right], \tag{4.34}$$

where $b_0(\vec{x})$ is the induction field created by a single bare vortex,

$$b_0(\vec{x})=\frac{\phi}{(2\pi)^2}\int d^2k\,e^{i\vec{k}\cdot\vec{x}}\frac{\lambda_L^{-2}C(\vec{k})}{\vec{k}^2+\lambda_L^{-2}C(\vec{k})}\,. \tag{4.35}$$

The magnetization $M(\vec{x})$ satisfies the nonlinear equation

$$M(\vec{x})=g\mu_BJNB_J\{(g\mu_BJ/k_BT)[b_0(\vec{x})+\tilde{\gamma}(-i\vec{\nabla})M(\vec{x})]\}\,. \tag{4.36}$$

Considerations outlined in Sec. II give the result that

$$\int d^3x\,E_{\rm core}(\vec{x})=\frac{\phi}{8\pi}\epsilon_1 \tag{4.37}$$

for a single vortex. This leads to

$$g_M(0)=b_0(0)+\epsilon_1+\frac{8\pi}{\phi}\int d^2x\left(\frac{1}{2}\vec{M}(\vec{x})\cdot\tilde{\gamma}(\vec{x})\vec{M}(\vec{x})-k_BTN\ln Z_J\{(g\mu_BJ/k_BT)\,|\,\vec{H}_m(\vec{x})\,|\,\}-F_m(\tilde{\gamma},0)\right). \tag{4.38}$$

The comparison calculated from (4.28) and (4.36) with (4.38) will be made in the next section.

When the superconductor is of the type II/1, $H(0)$ is not the lower critical field H_{c1}. In this case the critical flux density n_{c1} at H_{c1} is obtained by the largest value satisfying the equation

$$G_s(n_{c1})=G_s(0)\quad(\equiv G_M)\,. \tag{4.39}$$

Substituting (4.10) into (4.1), this condition is given by

$$n_{c1}^2\phi\frac{\partial g(n_{c1})}{\partial n_{c1}}=4\pi n_{c1}\phi m(\tilde{\gamma},n_{c1})+8\pi[F_m(\tilde{\gamma},n_{c1}\phi)-F_m(\tilde{\gamma}_P,0)]\,. \tag{4.40}$$

Then H_{c1} is obtained from (4.10)

$$H_{c1}=\frac{1}{2}\left[1+n_{c1}\frac{\partial}{\partial n_{c1}}\right]g(n_{c1})-4\pi m(\tilde{\gamma},n_{c1})\,. \tag{4.41}$$

When (4.40) has a solution other than $n_{c1}=0$, the first-order phase transition from the Meissner state to the mixed state occurs at H_{c1}, implying a type-II/1 superconductor. Equation (4.40) shows that the presence of the magnetic moments tends to help the system become type II/1, since the right-hand side of (4.40) does not exist in the nonmagnetic case.

From (4.14), (4.20), and (4.39), we can see that, if two of the three quantities H_{c2}, H_c^*, and H_{c1} are equal, then all three are equal:

$$\text{if } H_{c2}=H_c^*,\ \text{then}\ H_{c2}=H_{c1},\ldots\,. \tag{4.42}$$

D. The critical field H_P

In the above analysis, we assumed that all fields were along the third axis, that is in the direction of the applied field. However, for $T<T_P$, a periodic perpendicular component can appear when the applied field is sufficiently weak. The critical field H_P, where the conical spin alignment (spiral vortex) changes into parallel spin alignment, occurs at the same value of H for which the instability in the perpendicular spin susceptibility appears. Since $\vec{H}_m\|\vec{M}$, the perpendicular components of spins should satisfy

$$\vec{m}_0\times\vec{H}_{m\perp}+\vec{M}_\perp\times[\vec{h}_0+\gamma(\vec{0})\vec{m}_0]=0\,, \tag{4.43}$$

which leads to the equation

$$\{m_0\tilde{\gamma}(-i\vec{\nabla})-[n\phi+\tilde{\gamma}(\vec{0})m_0]\}\vec{M}_\perp=0\,. \tag{4.44}$$

Here $\vec{H}_m$ was given in (2.27).

When $\tilde{\gamma}(\vec{k})<[n\phi+\tilde{\gamma}(\vec{0})m_0]/m_0$, we have that $\vec{M}_\perp=0$. Therefore, a nonvanishing solution of $\vec{M}_\perp$ appears only for $n\le n_P$, with n_P determined by

$$\tilde{\gamma}(\vec{P})=[n_P\phi+\tilde{\gamma}(\vec{0})m(\tilde{\gamma},n_P\phi)]/m(\tilde{\gamma},n_P\phi)\,,$$
$$\tilde{\gamma}(\vec{P})=\max_{\vec{k}}\tilde{\gamma}(\vec{k})\,. \tag{4.45}$$

Then H_P is determined from (4.10).

V. NUMERICAL CALCULATION

Numerical calculations are performed by assuming that vortices form a triangle lattice with lattice constant a. Other possible lattice structures are not considered in this paper. The vortex density n is then given by

$$n=(2/\sqrt{3})/a^2 . \tag{5.1}$$

The magnitude of the reciprocal-lattice vectors is given by

$$K=2n\pi a(l^2+m^2-lm)^{1/2} , \tag{5.2}$$

where l and m are integers.

The nonlocal kernel $C(\vec{k})$ depends on ξ_0 (the coherence length at $T=0$) and $VN(0)$ with V being the BCS coupling constant and $N(0)$ the density of states at the Fermi level. When we have $0.2 \leq VN(0) \leq 0.4$, $C(\vec{k})$ is approximately given by[20]

$$C(\vec{k})=\exp\{-\nu[\bar{k}/\kappa(t)]^{\eta}\} , \tag{5.3}$$

$$\bar{k}=|\vec{k}|\lambda_L(t) , \tag{5.4}$$

$$\kappa(t)=[1/\gamma(t)][\lambda_L(t)/\lambda_L(0)]\kappa_B , \tag{5.5}$$

$$\nu=-0.4257VN(0)+0.559 , \tag{5.6}$$

$$\eta=-0.7857VN(0)+2.207 , \tag{5.7}$$

where κ_B is $\lambda_L(0)/\xi_0$ and t is the reduced temperature T/T_c with T_c denoting the superconducting transition temperature. The function $\gamma(t)$ is given by

$$\gamma(t)=1+at^n/(1-t)^m , \tag{5.8}$$

$$a=-0.0536VN(0)+0.3719 , \tag{5.9}$$

$$n=0.3714VN(0)+3.846 , \tag{5.10}$$

$$m=-0.0414VN(0)+0.550 . \tag{5.11}$$

The temperature dependence of the London penetration depth, $\lambda_L(t)/\lambda_L(0)$, on $t\,(=T/T_c)$ is calculated from the relation

$$\left[\frac{\lambda_L(0)}{\lambda_L(t)}\right]^2=1+2\int d\epsilon\frac{\partial f_E}{\partial E} , \tag{5.12}$$

where $f_E=[\exp(\beta E)+1]^{-1}$ with $E=[\epsilon^2+\Delta^2(t)]^{1/2}$, and $\Delta(t)$ is the fermion gap.

As a unit of length, we choose $\lambda_L(0)$. The magnetic field is scaled by $\phi/\lambda_L^2(0)$. Then we have following dimensionless parameters:

$$c=4\pi\Theta_C/T_m , \tag{5.13}$$

$$d=D/T_m\lambda_L^2(0) , \tag{5.14}$$

$$u=g\mu_B JN/[\phi/\lambda_L^2(0)] . \tag{5.15}$$

The last parameter signifies the strength of the magnetic moment in terms of the unit flux. Notations of the physical parameters and the dimensionless parameters are summarized in Table I.

Scaling the magnetic field by $[\phi/\lambda_L^2(0)]$, $H_c^2/8\pi$ is given by

$$\frac{H_c^2}{8\pi}=\frac{3\kappa_B^2}{16\pi^5}\left[\frac{H_c(t)}{H_c(0)}\right]^2\left[\frac{\phi}{\lambda_L^2(0)}\right]^2 . \tag{5.16}$$

The temperature dependence of $H_c(t)/H_c(0)$ is calculated from

$$\left[\frac{H_c(t)}{H_c(0)}\right]^2=\left[\frac{\Delta(t)}{\Delta(0)}\right]^2 -\frac{2\pi^2}{3}\left[\left[\frac{1}{1.764}\right]^2t^2-\frac{\pi^2}{6\Delta^2(0)} \times\int_0^{\infty}d\epsilon\left[\frac{\epsilon^2+E^2}{E}\right]f_E\right] . \tag{5.17}$$

To make our problem concrete, we consider $ErRh_4B_4$ and $HoMo_6S_8$. The experimental values of relevant physical quantities are summarized in Table II. Some of the values show a certain amount of

TABLE I. Notations of physical parameters and dimensionless parameters.

Physical parameters	
T_c (or T_{c1})	Superconducting transition temperature
T_{c2}	Reentrant temperature
T_P	Periodic phase transition temperature
T_M	(Fictitious) reentrant temperature from Meissner to normal state
T_m	(Fictitious) Curie temperature of the normal phase
Θ_C	Curie constant
D	Stiffness constant
J	Spin of rare-earth ions
N	Density of the rare-earth ions
$\lambda_L(0)$	London penetration depth at $T=0$ K
$\xi(0)$	Coherent length at $T=0$ K
Dimensionless parameters	
t	T/T_c
t_P	T_P/T_c
t_M	T_M/T_c
t_m	T_m/T_c
κ_B	Landau parameters $[\xi(0)/\lambda_L(0)]$
c	$4\pi\Theta_C/T_m$
d	$D/T_m\lambda_L^2(0)$
u	$g\mu_B JN/[\phi/\lambda_L^2(0)]$

TABLE II. Experimental values.

	$ErRh_4B_4$	$HoMo_6S_8$
Crystal structure	Tetragonal[a]	Rhombohedral[b]
	$a=5.30$ Å	$a=6.45$ Å
	$c=7.39$ Å	$\alpha\sim 89.5°$
	$N=9.64\times 10^{22}/cm^3$	$N=3.726\times 10^{22}/cm^3$
$J_{(free)}$	$\frac{15}{2}$	8
$\mu_{(free)}$	9.59	10.60
$\mu_{(eff)}^{expt}$	5.6 (neutron)[c]	9.06 (neutron)[d]
	8.4 (Mössbauer)[e]	
	9.62 (χ^{-1}, high T)[f]	6.0 (high field)[g]
	7.65 (χ^{-1}, high field)[h]	10.85 (χ^{-1}, high T)[g]
T_{c1}	8.7 K[f,h,i]	1.82 K[g,j]
T_{c2}	0.93 K (warming)[i]	0.668 (warming)[j]
	0.87 K (cooling)[i]	0.612 (cooling)[j]
Single		
	0.775 K (warming)[k]	
	0.710 K (cooling)[k]	

[a]Reference 23.
[b]Reference 24.
[c]Reference 25.
[d]Reference 26.
[e]Reference 27.
[f]Reference 1.
[g]Reference 2.
[h]Reference 28.
[i]Reference 29.
[j]Reference 30.
[k]Reference 31.

scatter, depending on the sample and the experimental method. In Table III, we present our tentative choice for the values of the various physical quantities. Since the discrepancy among the observed saturation moments is not fully understood, we make use of the values of the magnetic moment of free rare-earth ions. The detailed nature of the transition mechanism around the reentrant point T_{c2} is not completely resolved although it is known to be first order. Furthermore, most of the experimental values in Table II are obtained from polycrystalline samples, while our theoretical analysis is based on the assumption of a single crystal. From Table III we obtain the values of theoretical parameters given in Table IV. Parameters d and u cannot be determined unless we know the stiffness constant D of the staggered susceptibility in the normal state and the London penetration depth $\lambda_L(0)$. In the most of present analysis, d and u are determined in such a way that a particular value of t_P ($\equiv T_P/T_c$) and t_M are obtained. With t_P and t_M fixed, d and u are no longer free parameters. A signal of periodic ordering in the neutron scattering has been observed in $ErRh_4B_4$ (Ref. 32) around 1—0.7 K and in $HoMo_6S_8$ (Ref. 33) around 0.7—0.6 K. Both exhibit a strong thermal hysteresis. This seems to indicate the occurrence of a spin-sinusoidal order in $HoMo_6S_8$ and $ErRh_4B_4$.[31]

Before presenting various phase diagrams in the H-T plane, it is worthwhile to point out a need of careful calculation of $H(n=0)$ at $t\sim t_P$. The value of $H(n=0)$ obtained from the linear approximation [i.e., (4.28)] will be called $H_l(0)$, while that obtained from a self-consistent calculation using (4.33) together with (4.36) and (4.38) will be called $H_s(0)$. As was pointed out previously, $H_l(0)$ obtained from (4.28) is the same one given in Ref. 3 and is not a good approximation when T is close to T_P; as a

TABLE III. Parameters used in calculation.

	$ErRh_4B_4$	$HoMo_6S_8$
T_{c1}	8.7 K	1.82 K
T_{c2} $(=T_M)$	0.93	0.67
T_P	1.2 or 0.7	0.7
T_m	1.4	0.8
J	$\frac{15}{2}$	8
gJ	9	10
N	9.64×10^{23}	3.726×10^{23}
Θ_c	0.184 K	0.087 K

TABLE IV. Reduced parameters.

	$ErRh_4B_4$	$HoMo_6S_8$
t_M	0.11	0.37
t_P	0.14 or 0.08	0.38
t_m	0.16	0.44
c	1.6	1.4

matter of fact, $H_l(0)$ goes to $-\infty$ as T approaches T_P. Therefore, when T is close to T_P, we must solve the nonlinear equation (4.36) which includes the saturation effect. Equation (4.36) can be solved by approximating $\tilde{\gamma}(\vec{k})$ as

$$\tilde{\gamma}(\vec{k})=\frac{T_m}{\Theta_C}\exp\left[-\frac{Dk^2}{T_m}\right]-4\pi\frac{\lambda_L^{-2}\tilde{C}_k}{k^2+\lambda_L^{-2}\tilde{C}_k}\ , \tag{5.18}$$

where $k=|\vec{k}|$ and

$$\tilde{C}_k=\frac{1}{1+\alpha[\bar{k}/\kappa(t)]^2}\ ,\quad \alpha=0.4468\ . \tag{5.19}$$

Here and in the following, we use $VN(0)=0.2635$, because the results are relatively insensitive to our choice of $VN(0)$ and because the choice $VN(0)=0.2635$ simplifies the calculation [it gives $\eta=\frac{1}{2}$ in (5.3)]. The approximation (5.18) enables us to make an exact calculation of the kernel $\tilde{\gamma}(-i\vec{\nabla})$ in configuration space, which considerably simplifies our numerical calculation. Although the $C(\vec{k})$ in $\tilde{\gamma}(\vec{k})$ is approximated by $\tilde{C}_k$, we used the form (5.3) for the c function in $b_0(\vec{x})$ in (4.36). The self-consistent calculation is performed at forty points

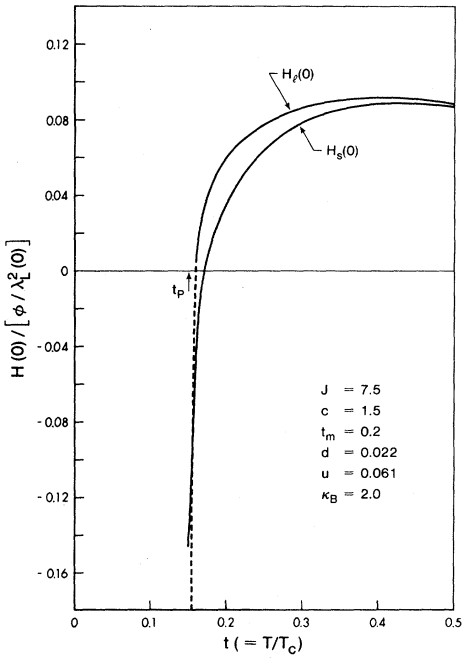

FIG. 1. Comparison of the linear approximation and nonlinear approximation (self-consistent calculation) for the calculation of $H(n=0)$ as a function of the reduced temperature. The $H_l(0)$ denotes the linear approximation which is the same one in Ref. 3 while $H_s(0)$ denotes the self-consistent numerical calculation. The difference comes from the saturation effect. Parameters are chosen as $VN(0)=0.2635$, $\kappa_B=2.0$, $J=7.5$, $c=1.5$, $t_m=0.30$, $d=0.022$, and $u=0.061$, which give $t_P=0.15$ and $t_M=0.10$.

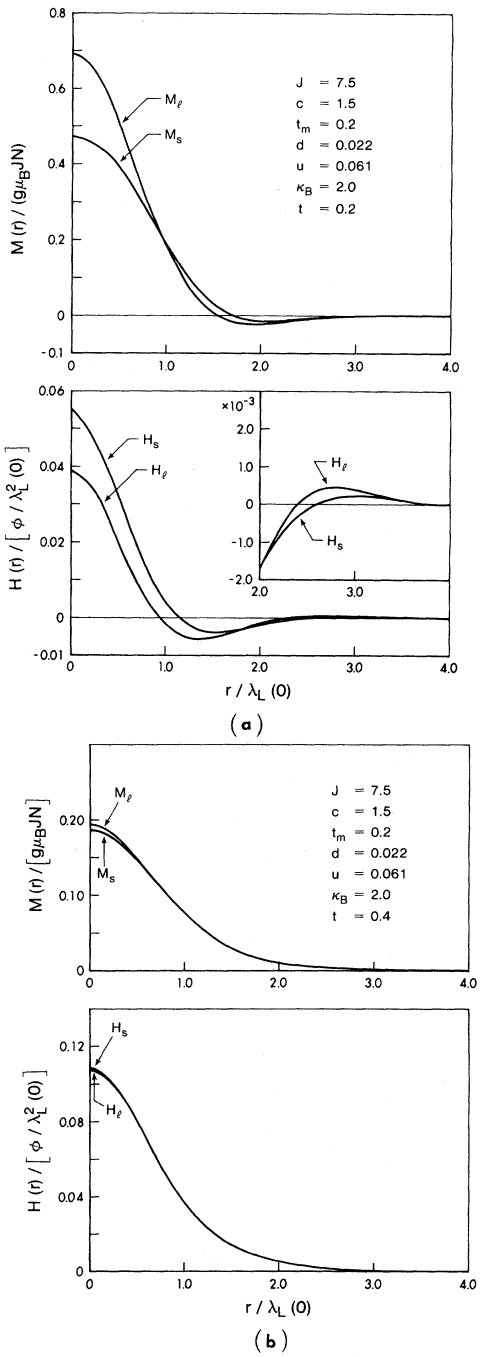

FIG. 2. Spatial dependence of the magnetic field and magnetic moment due to a single vortex. The subscript l indicates the linear approximation which is the same one in Ref. 3, while s indicates the self-consistent calculation including the saturation effect. (a) is at $t=0.2$ and (b) is at $t=0.4$. Parameters are the same as those in Fig. 1.

between $r/\lambda_L=0$ and 8. In Fig. 1, the calculated $H_s(0)$ and $H_l(0)$ are presented for the parameters $VN(0)=0.2635$, $\kappa_B=2.0$, $J=7.5$, $c=1.5$, $t_m=0.2$, $t_P=0.15$, and $t_M=0.10$ (in this case $d=0.022$ and $u=0.061$). Note that $H_l(0)$ is obtained by the same approximation as in Ref. 3 [see (4.28)]. The corresponding spatial dependence of $M(x)$ and $H(x)$ is illustrated in Fig. 2(a) ($t=0.2$) and Fig. 2(b) ($t=0.4$). The subscript l refers to the results of the linear approximation, while s refers to the results of the self-consistent calculation. The results show that the linear approximation is qualitatively reasonable provided t is not close to t_P. The $H_s(0)$ is finite at T_P, though $H_l(0)$ is negatively infinite. Therefore, in the following we use only the linear approximation and avoid the very small domain of t around t_P. At $t=t_P$, we calculate $H_s(0)$. In this way we can study the overall behavior of $H(n=0)$ as a function of t

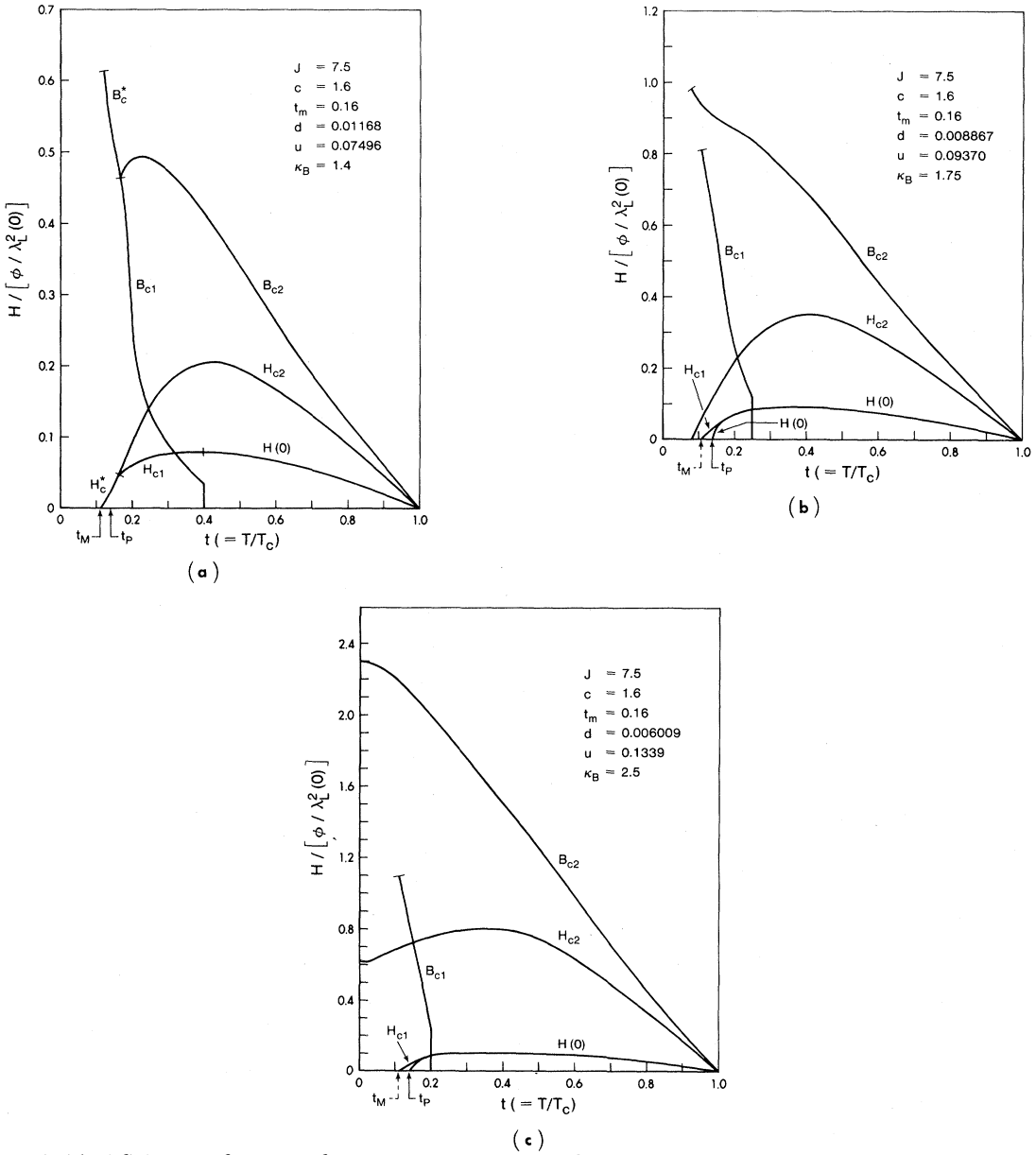

FIG. 3. Critical fields as a function of the reduced temperature for $t_P>t_M$ case with low t_m. Parameters are chosen as $VN(0)=0.2635$, $J=7.5$, $c=1.6$, $t_m=0.16$, $t_P=0.14$, and $t_M=0.11$. (d,u) are calculated for each κ_B. The bars indicate the various phase transition points. (a) is for $\kappa_B=1.4$, $d=0.011\,68$, $u=0.074\,96$, and $H_s(0)/[\phi/\lambda_L^2(0)]$ at $t_P=-0.037$. (b) is for $\kappa_B=1.75$, $d=0.008\,867$, $u=0.093\,70$, and $H_s(0)/[\phi/\lambda_L^2(0)]$ at $t_P=-0.089$. (c) is for $\kappa_B=2.5$, $d=0.006\,009$, $u=0.1339$, and $H_s(0)/[\phi/\lambda_L^2(0)]$ at $t_P=-0.189$.

$(=T/T_c)$. As the vortex density n is increased, the linear approximation, mentioned in Sec. IV, is expected to improve.

As is seen in Fig. 2(a), the attractive dip of $H(r)$ around $r=1.5\lambda_L(0)$ is of the order 10^{-2}, while the repulsive tail near $r/\lambda_L(0)\sim 3.0$ is of the order 10^{-3}. To understand the significance of this small repulsive tail, we note that the attractive dip in nonmagnetic superconductors such as Nb is only of the order 10^{-5} in units of $\phi/\lambda_L^2(0)$,[34] although it is strong enough to make Nb a type-II/1 superconductor.

In Figs. 3–7, we present several examples of phase diagrams in the H-T plane. In each figure,

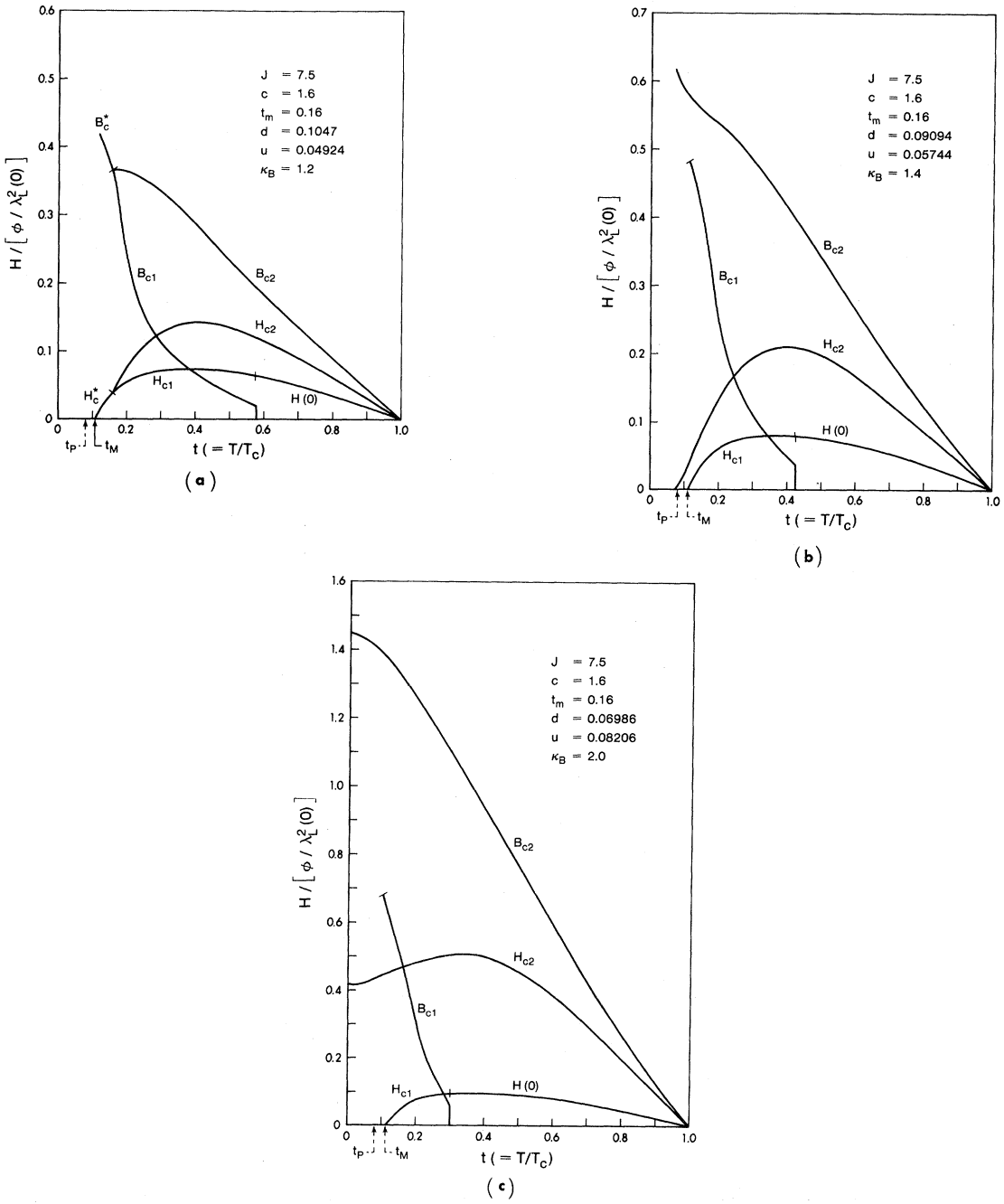

FIG. 4. Critical fields as a function of the reduced temperature for the $t_P < t_M$ case with low t_m. Parameters are chosen as $VN(0)=0.2635$, $J=7.5$, $c=1.6$, $t_m=0.16$, $t_P=0.08$, and $t_M=0.11$. (d,u) are calculated for each κ_B. The bars indicate the various phase transition points. (a) $\kappa_B=1.2$, $d=0.1047$, $u=0.04924$; (b) $\kappa_B=1.4$, $d=0.09094$, $u=0.05744$; (c) $\kappa_B=2.0$, $d=0.06986$, $u=0.08206$.

the critical magnetic fields H_{c2}, H_c^*, H_{c1}, and $H(n=0)$ along with the critical flux densities B_{c2}, B_c^* and B_{c1} are illustrated. We have presented the results of the critical flux density calculations because they yield significant information regarding the spin degrees of freedom in magnetic superconductors. In particular, it is predicted that the behavior of the critical flux densities resembles that of the critical field in nonmagnetic superconductors, assuming the s-f interaction is weak.[35] This point

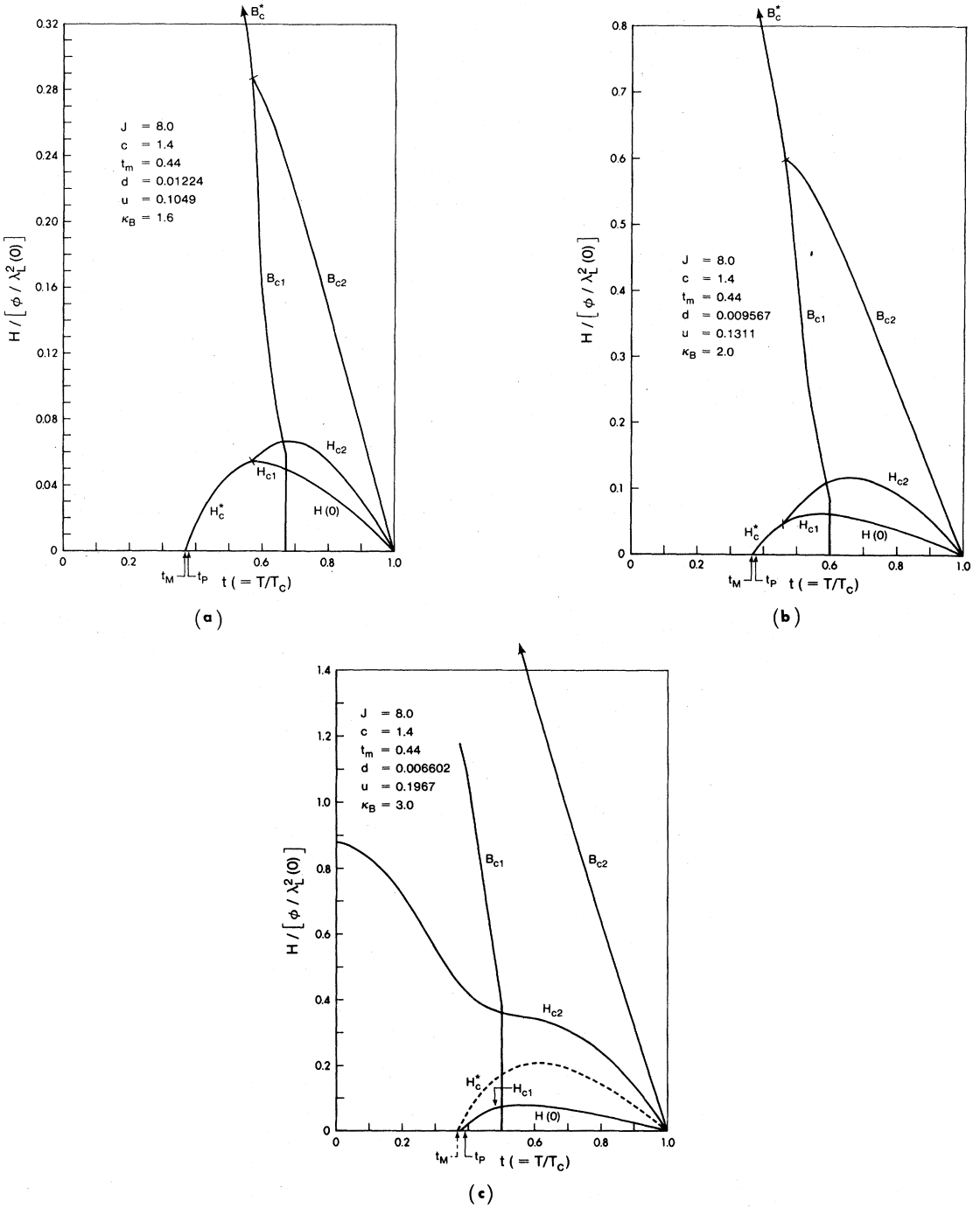

FIG. 5. Critical fields as a function of the reduced temperature for the $t_P > T_M$ case with higher t_m. Parameters are chosen as $VN(0)=0.2635$, $J=8.0$, $c=1.4$, $t_m=0.44$, $t_P=0.38$, and $t_M=0.37$. (d,u) are calculated for each κ_B. The bars indicate the various phase transition points. (a) $\kappa_B=1.6$, $d=0.012\,24$, $u=0.1049$; (b) $\kappa_B=2.0$, $d=0.009\,567$, $u=0.009\,567$; (c) $\kappa_B=3.0$ $d=0.006\,602$, $u=0.1967$.

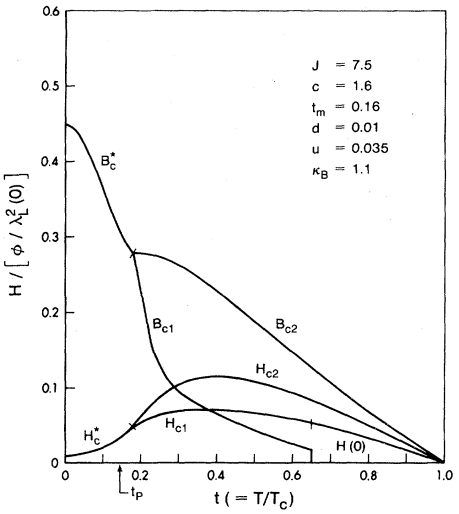

FIG. 6. Critical fields as a function of the reduced temperature for a case without t_M. t_m is chosen to be as low as 0.16. Other parameters are $VN(0)=0.2635$, $J=7.5$, $c=1.6$, $u=0.035$, $d=0.01$, $\kappa_B=1.1$, $t_P=0.1461$, and $H_s(0)/[\phi/\lambda_L^2(0)]$ at t_P is 0.025. The bars indicate the various phase transition points.

was not recognized in Ref. 3. Figures 3 and 4 are for smaller values of t_m. Figure 3 is for $t_P > t_M$ while Fig. 4 is for $t_P < t_M$. Figure 5 is for rather larger values of t_m and $t_P > t_M$. Figures 6 and 7 illustrate some examples in which no reentrant temperature t_M exists; Fig. 6 is for the smaller values of t_m, while Fig. 7 is for the larger values of t_m. The

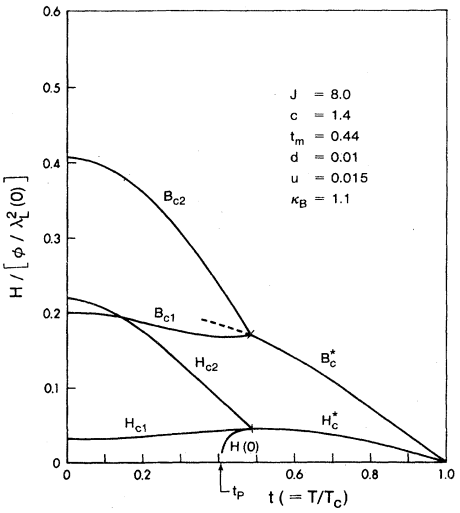

FIG. 7. Critical fields as a function of the reduced temperature for a case without t_M. t_m is chosen to be as high as 0.44. Other parameters are $VN(0)=0.2635$, $J=8.0$, $c=1.4$, $u=0.015$, $d=0.01$, $\kappa_B=1.1$, and $t_P=0.4041$. The bars indicate the various phase transition points.

parameters are chosen from Table IV. All the examples considered here have critical temperature t_P, although it may not be observable when $t_P < t_M$ or when some phase other than the spin-periodic phase is favored. There are choices of parameters, for which t_P does not appear, although no example of this kind is presented. The behavior of the critical fields in this case is very similar to the ones for which $t_P < t_m$. In the calculation in Ref. 3 we did not consider $t < t_m$, since the linear approximation used in Ref. 3 would have been inappropriate in the consideration of normal state at $t < t_m$. Since t_P and t_m are always smaller than t_m, those critical temperatures are only meaningful, in the comparison of the free energies, when the nonlinear (or saturation effect) is considered.

As one can see from Figs. 3 and 4, the overall behavior of the critical fields, other than H_c^*, is not sensitive to the ordering between t_P and t_M. However, the behavior of H_c^* for $t_P > t_M$ is quite different from that for $t_P < t_M$. As is seen from Figs. 3(a) and 6, the H_c^* curve has a positive curvature below t_P and a negative curvature above t_P; i.e., t_P is an inflection point. The values of H_c^* below t_P and t_M indicated in Figs. 3–7 are calculated using the isotropic approximation, that is for the spiral phase. The decrease of H_c^* with decreasing temperature is caused by the decrease of the free energy of spin system in the normal state. When $t_P > t_M$, the spin-spiral ordering appears in the Meissner state below t_P. As a result, there appears a change of slope of H_c^* at t_P and the decrease in H_c^* is reduced. When the system favors the spin-sinusoidal structure, H_c^* is determined approximately using Eq. (4.26). For the same parameters (d, u, and c) the H_c^* curve below t_P in Fig. 3(a), for example, is reduced, as shown in Fig. 8.

While the value of t_P is sensitive to the value of d chosen, this is not the case in the behavior of H_{c2} provided $d < 0.1$. Therefore, the choice of parameters, $t_P < t_M$ or $t_P > t_M$, does not greatly affect the overall behavior of H_{c2}.

The critical field H_{c2} is considerably reduced by the magnetic effects, which depend on t_m, u, and κ_B. However, the modification of $n_c\phi$ due to the magnetic moment, which is denoted by B_{c2} in the figures, is much milder than that of H_{c2}. Briefly speaking, when $T \simeq T_c$, B_{c2} is not much different from its value for the nonmagnetic one, while the upper critical field H_{c2} is considerably modified by the magnetic moment by the relation[35]

$$(1+4\pi\chi)H_{c2}=B_{c2} \quad \text{for } T \cong T_c\ , \tag{5.20}$$

where χ is the static susceptibility.

In most examples in which the reentrant phenomena takes place (i.e., $T_M > 0$), H_{c2} decreases with de-

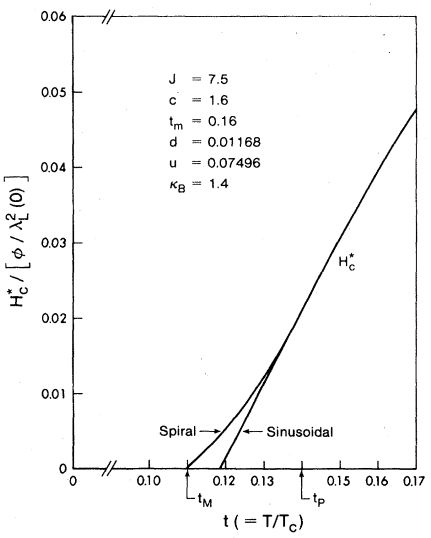

FIG. 8. Comparison of H_c^* as a function of the reduced temperature below t_p between spin-spiral phase and sinusoidal phase. Parameters are $VN(0)=0.2635$, $J=7.5$, $c=1.6$, $t_m=0.16$, $t_P=0.14$, $t_M=0.11$, and $\kappa_B=1.4$ ($d=0.01168$, $u=0.07496$).

creasing temperature in the low-temperature domain. The reduction of H_{c2} is enhanced for larger values of u. However, there are exceptions. When the competition between B_{c2} and $4\pi M_{c2}$ is intricate, the curve of H_{c2} ($\equiv B_{c2}-4\pi M_{c2}$) sometimes shows a dip and bump [Fig. 5(c)].

When κ_B is small, the transition from the type II to type I is observed with decreasing temperature [Figs. 3(a), 4(a), 5(a), 5(b), and 6].[36] Figure 6 shows an example of the behavior of H_c^* when the reentrant phenomena does not take place and the superconductor becomes type I at low temperature. In some rare cases (Fig. 7), the transition from type I to type II is also possible with decreasing temperature. The mechanism for this can be understood in the following way. As was discussed in Ref. 27 at T near T_c, the effect of the magnetic moment is roughly taken into account by the rescaling of κ_B:

$$\kappa_B' = \frac{\kappa_B}{[1+4\pi\chi(t)]^{1/2}} . \tag{5.21}$$

Therefore, when χ is large enough to satisfy $\kappa_B' \leq 1/\sqrt{2}$ for $t \simeq t_c$ (this happens, for example, when T_m is very close to T_c), the superconductor becomes type I at T near T_c. This is the case for Fig. 7. When the temperature is reduced, the critical vortex density n_c and the polarization of the localized spin $4\pi M_{c2}$ increases, resulting in decrease of χ. Then, according to the scaling relation (5.21), κ_B' increases and the superconductor changes into a type-II superconductor.

Let us now consider those cases in which the system is of type II for $t \simeq t_c$. As was discussed in Ref. 3, the effect of the spin fluctuation $\chi(\vec{k})$ enhances the attractive interaction of the intervortex interaction. This tends to favor a first-order transition in the magnetization. The transition from a type-II/2 to type-II/1 superconductor occurs at a certain temperature in all the examples considered. This temperature corresponds to the sudden appearance of B_{c1} which also corresponds to the boundary between H_{c1} and $H(n=0)$ indicated by the vertical bar in Figs. 3(a)–3(c), 4(a)–4(c), 5(a)–5(c), and 6. For lower κ_B, this transition temperature is higher, since the lower value for κ_B favors the type-II/1 behavior. When this attractive interaction becomes strong enough, the superconductor makes the phase transition into a type-I superconductor. This is seen in Figs. 3(a), 4(a), 5(a), 5(b), and 6. When κ_B is increased, the ratio $B_{c2}/4\pi M_{c2}$ also increases. When this ratio becomes unity, reentry to the normal state at $H=0$ through the mixed state takes place [Figs. 3(b), 4(b)]. In this case, the reentrant phase transition is second order. When κ_B is further increased, the system is a type-II superconductor in the entire temperature range below T_c (i.e. type-I phase does not appear), and H_{c2} has a minima in the low-temperature region [Figs. 3(c), 4(c) and 5(c).

In the case of Figs. 6 and 7, the system is superconducting at $H=0$ in the entire temperature range below T_c; i.e., T_M does not appear. Depending on whether a type-II→type-I transition occurs or not, the phase transition to the normal state is either first or second order for fixed H with changing temperature.

As was pointed out previously, variation of the critical flux density B_{c2} due to the magnetic moment is much weaker than the variation of H_{c2}. In fact, there is practically no change in B_{c2} at T near T_c, as was pointed out in Ref. 35. However, near the point where the type-II→type-I transition takes place, B_{c2} shows a considerable reduction [Figs. 3(a), 4(a), 5(a), 5(b), and 6].

It is worth pointing out that the H_{c2} curve in Fig. 3(a) or 4(a) has a behavior very similar to the one observed in $ErRh_4B_4$ (Refs. 28 and 36) and that of Fig. 5(b) resembles the one observed in $HoMo_6S_8$.[2] To see if these resemblances are meaningful or not, we need to know the real values of various physical parameters, in particular the value of κ_B.

Figure 9 shows typical examples of the magnetization curve. In Fig. 9(a), we consider a particular case as a model for $ErRh_4B_4$. In this case we have $t_P > t_M$. A similar case with $t_P < t_M$ is presented in Fig. 9(b). The points at which the dotted lines begin indicate the transition from the mixed state to the

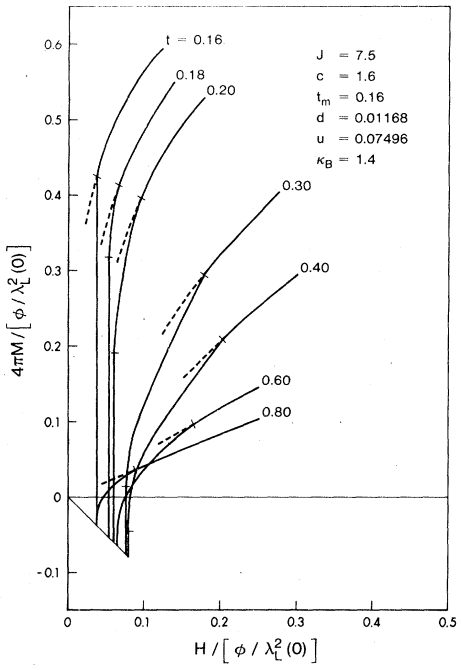

FIG. 9. Magnetization curve. (a) is for $VN(0)=0.2635$, $J=7.5$, $c=1.6$, $t_m=0.16$, $t_P=0.14$, $t_M=0.11$, $\kappa_B=1.4$; (b) is for $VN(0)=0.2635$, $J=7.5$, $c=1.6$, $t_m=0.16$, $t_P=0.08$, $t_M=0.11$, $\kappa_B=1.2$. The parameter t is the reduced temperature T/T_c. The points at which the dotted lines begin indicate the transitions from the mixed state to the normal state. The first-order transition from the Meissner state to the mixed state (i.e., type II/1) is indicated by the horizontal bars.

normal state. The first-order transition from the Meissner state to the mixed state (i.e., type II/1) is indicated by the horizontal bars. The observed temperature behavior of the magnetization for $ErRh_4B_4$ is very similar to the curve shown in Fig. 9.[28] As was mentioned in Ref. 3, the increase in the magnetization near $H(0)$ is very rapid even in type-II/2 region. [See Fig. 9(a), $t=0.8,0.6$.] Despite the occurrence of the type-II/2→type-II/1 transition at $t=0.4$ in Fig. 9(a), it is very difficult to distinguish between the $t=0.6$ and $t=0.4$ cases. This suggests that it may be difficult to identify the transition from type II/2 to type II/1 experimentally from the magnetization measurement, unless one studies the hysteresis properties.

The original type-II/1 magnetization curve obtained consists of wavy curves as shown in Fig. 10. This wavy behavior is a result of the oscillatory nature of the intervortex interaction $h(r)$ in Fig. 2. Figure 9 shows the results for an infinite system and in this case, the wavy behavior disappears and a first-order transition appears. When one considers the demagnetizing effect of the finite sample, this wavy behavior of the magnetization curve may become observable. [Even in the nonmagnetic case for small κ ($>1/\sqrt{2}$), this kind of behavior may exist but is very small.]

When H_{c1} becomes zero with decreasing temperature, the self-induced vortex state is realized without any external field (i.e., $H=0$). This example is shown in Fig. 4(b). In Fig. 11, the magnetization curve for this case was illustrated. The transition to the self-induced vortex state through decreasing temperature is usually a first-order transition. The appearance of the self-induced vortex state can be understood intuitively by the mechanism in which the spin polarization supports the vortices in a manner similar to the external magnetic field. The criterion for the stability of this state at $T=0$ is examined in Ref. 9 (see also Refs. 10 and 37).

Although in most cases the transition to the self-induced vortex state is first order, there exists the very slim possibility for a second-order transition. The second-order transition into the self-induced vortex state is possible, when and only when $H(0)$ is smaller than H_{c1} at the transition temperature. Here H_{c1} denotes the critical field at which the first-order phase transition takes place from the Meissner state to the mixed state. $H(0)$ must vanish at the transition temperature, below which $H(0)$ is negative. In the context of our approximation, it is hard to decide whether or not $H(0)$ could be negative, since a very precise calculation of $H(0)$ at $t\simeq t_P$ requires a much better calculation than our self-consistent calculation. The fact that our self-consistent calculation gives a negative value for

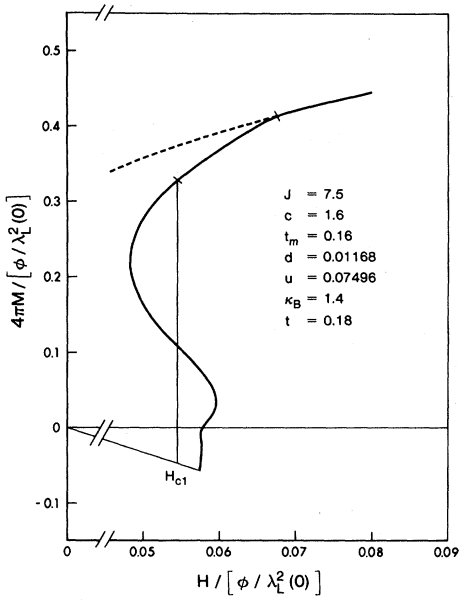

FIG. 10. Magnetization curve of the mixed state (type II/1). The first-order transition takes place at H_{c1}.

$H_s(0)$ [Figs. 3(a)—3(c)] is therefore not conclusive.

We point out that, when $H(0)$ is smaller than H_{c1}, a first-order jump in the magnetization can appear

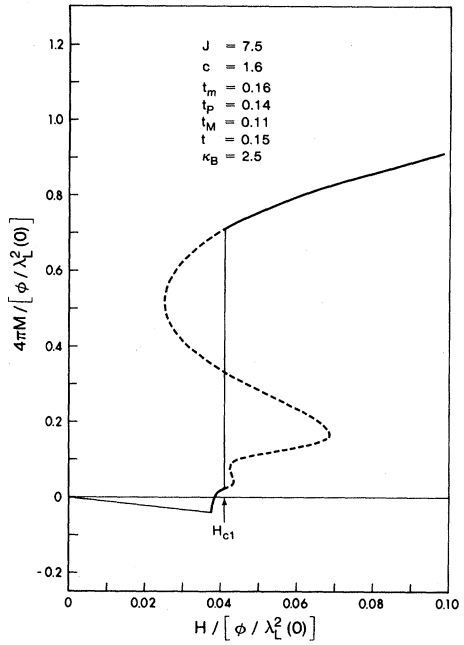

FIG. 12. Magnetization curve for the first-order transition from the mixed state (type II/3). Parameters are $VN(0)=0.2635$, $J=7.5$, $c=1.6$, $t_m=0.16$, $t_P=0.14$, $t_M=0.11$, $\kappa_B=2.5$ ($d=0.006009$, $u=0.1339$), and $t=0.15$.

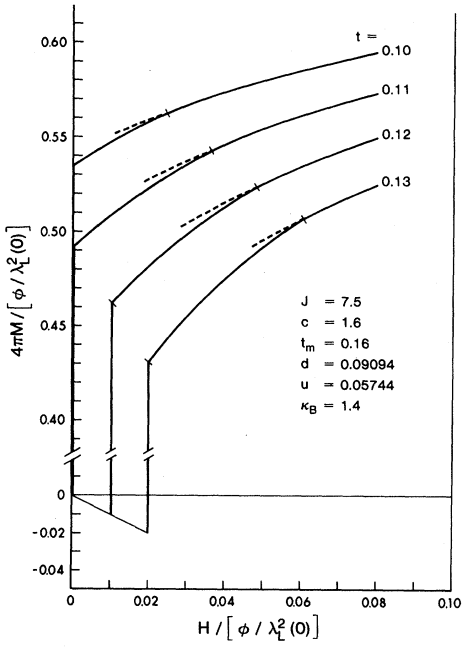

FIG. 11. Magnetization curve for the case where first-order self-induced vortex state occurs. Parameters are $VN(0)=0.2635$, $J=7.5$, $c=1.6$, $t_m=0.16$, $t_P=0.08$, $t_M=0.11$ ($d=0.09094$, $u=0.05744$), and $\kappa_B=1.4$. The parameter t is the reduced temperature T/T_c.

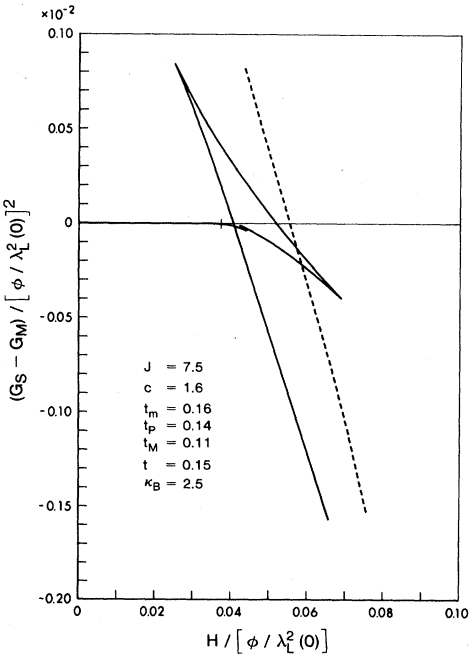

FIG. 13. The free-energy behavior of type II/3. Parameters are $VN(0)=0.2635$, $J=7.5$, $c=1.6$, $t_m=0.16$, $t_P=0.11$, $t_M=0.11$, $\kappa_B=2.5$, and $t=0.15$. The solid line is for the mixed state and the dashed line is for the normal state.

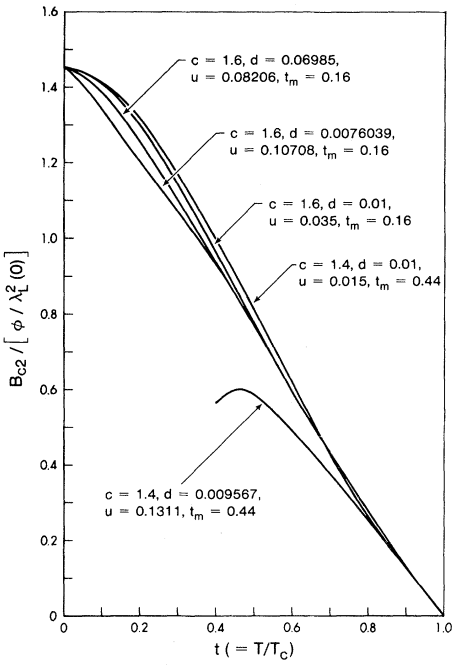

FIG. 14. Behavior of the critical flux B_{c2} as a function of the reduced temperature. The κ_B is fixed to be 2.0.

in the middle of the mixed state as is seen from the result for the $t=0.15$ case in Fig. 12. The behavior of the free energy is also illustrated in Fig. 13. In general, when the first-order transition from a mixed state takes place, we call such a superconductor type II/3. This transition is caused by the oscillation of the intervortex potential. Note that this oscillation is enhanced when T is close to T_P.

Finally in Fig. 14, we show the B_{c2} behavior for various parameters for the same value of κ_B ($=2.0$). As can be seen from the figure, the parameter dependence is milder, although H_{c2} depends drastically on the choice of parameters. At T, very near T_c, the dependence of B_{c2} on the parameters is practically negligible. At lower temperatures, however, a mild dependence becomes observable. This numerical result is consistent with Ref. 35 in which the rescaling procedure of κ_B was proposed.

VI. CONCLUSIONS

Here we summarize the main results of this paper:

(1) We found many types of phase changes in the magnetic properties. With decreasing temperature, depending on the parameters, we have

(a) type II/2→type II/1→type I→reentrant [Figs. 3(a), 4(a), 5(a), 5(b)],

(b) type II/2→type II/1→self-induced→reentrant [Figs. 3(b), 4(b)],

(c) type II/2→type II/1→self-induced (no reentrant) [Figs. 3(c), 4(c), 5(c)],

(d) type II/2→type II/1→type I (no reentrant) (Fig. 6),

(e) type II/2→type II/1 (no reentrant) (not shown in figures),

(f) type I→type II/1 (no reentrant) (Fig. 7).

(2) For certain choices of the parameters there appears a periodic phase in the Meissner state. [Such a phase, for example, appears in Fig. 3(a) but it does not in Fig. 4(a).]

(3) The reentrance to the normal state from the superconducting state is first order when it is from the Meissner state and second order when it is from the mixed state (i.e., from the self-induced vortex state).

(4) A typical magnetization curve, showing the temperature dependence of the magnetization, is presented in Figs. 9(a) and 9(b).

(5) A possibility of the type II/3 is pointed out.

(6) It is shown numerically that, when the s-f interaction is neglected, the parameter dependence (other than κ_B) of the critical flux B_{c2} is rather mild. However B_{c2} diminishes considerably at the temperature around the transition type II→type I.

[1]W. A. Fertig, D. C. Johnston, L. E. Delong, R. W. McCallum, M. B. Maple, and B. T. Matthias, Phys. Rev. Lett. 38, 987 (1977).

[2]M. Ishikawa and Ø. Fisher, Solid State Commun. 23, 37 (1977); 24, 747 (1977).

[3]M. Tachiki, H. Matsumoto, and H. Umezawa, Phys. Rev. B 20, 1915 (1979).

[4]T. Jarlborg, A. J. Freeman, and T. J. Watson-Yang, Phys. Rev. Lett. 39, 1032 (1977); A. J. Freeman and T. Jarlborg, J. Appl. Phys. 50, 1876 (1979); 44, 178 (1980).

[5]H. Matsumoto, H. Umezawa, and M. Tachiki, Solid State Commun. 31, 157 (1979); M. Tachiki, A. Kotani, H. Matsumoto, and H. Umezawa, *ibid.* 31, 927 (1979).

[6]See also E. I. Blout and C. M. Varma, Phys. Rev. Lett. 42, 1079 (1979).

[7]M. Tachiki, A. Kotani, H. Matsumoto, and H. Umezawa, Solid State Commun. 32, 599 (1979).

[8]This possibility has been pointed out by B. T. Matthias and H. Suhl, Phys. Rev. Lett. 4, 51 (1960).

[9]M. Tachiki, H. Matsumoto, T. Koyama, and H.

Umezawa, Solid State Commun. 34, 19 (1980).
[10]C. G. Kuper, M. Revzen, and A. Ron, Phys. Rev. Lett. 44, 1545 (1980). (Note that their consideration is for the case where a single vortex is created spontaneously.)
[11]M. Tachiki, A. Kotani, S. Takahashi, T. Koyama, H. Matsumoto, and H. Umezawa, Solid State Commun. 37, 113 (1981); A. Kotani, S. Takahashi, M. Tachiki, H. Matsumoto, and H. Umezawa, Solid State Commun. 37, 619 (1981); A. Kotani, M. Tachiki, H. Matsumoto, and H. Umezawa, Phys. Rev. B 23, 5960 (1981).
[12]M. Tachiki, S. Takahashi, H. Matsumoto, and H. Umezawa, Solid State Commun. 32, 393 (1980).
[13]M. Tachiki, T. Koyama, H. Matsumoto, and H. Umezawa, Solid State Commun. 34, 269 (1980).
[14]S. C. Schneider, M. Levy, R. Chan, M. Tachiki, D. C. Johnston, and B. T. Matthias, Solid State Commun. 40, 61 (1981); N. Toyota, Y. Muto, and S. B. Woods, *ibid.* 37, 547 (1981).
[15]O. Sakai, M. Tachiki, H. Matsumoto, and H. Umezawa, Solid State Commun. 39, 279 (1981).
[16]By use of the Ginzburg-Landau theory, the behavior of the magnetic field with the presence of the magnetic moments is investigated by W. Krey, Int. J. Magn. 3, 65 (1972); 4, 153 (1973).
[17]By starting from the view point of two competing magnetizations from the superconducting system and the spin system, M. V. Jarić also discussed the phase diagrams in H-T plane; M. V. Jarić and M. Belic, Phys. Rev. Lett. 42, 1015 (1979); M. V. Jarić, Phys. Rev. B 20, 4486 (1979).
[18]L. Leplae, F. Mancini, and H. Umezawa, Phys. Rep. 10C, 151 (1974).
[19]H. Matsumoto, M. Tachiki, and H. Umezawa, Fortschr. Phys. 25, 273 (1977).
[20]I. Shapira, M. N. Shah, and H. Umezawa, Physica B84, 213 (1976).
[21]F. Mancini, M. Tachiki, and H. Umezawa, Physica B94, 1 (1978).
[22]D. K. Christen, S. Spooner, P. Thorel, and H. R. Kerchner, J. Appl. Crystallog. 11, 650 (1978); 11, 654 (1978).
[23]J. M. Vandenberg and B. T. Matthias, Proc. Natl. Acad. Sci. USA 74, 1336 (1977).
[24]K. Yvon, in *Current Topics in Materials Science,* edited by E. Kaldis (North-Holland, Amsterdam, 1979), Vol. III, p. 53.
[25]D. E. Moncton, D. B. McWham, J. Eckert, G. Shirane, and W. Thomlinson, Phys. Rev. Lett. 39, 1164 (1977).
[26]J. W. Lynn, D. E. Moncton, W. Thomlinson, G. Shirane, and R. N. Shelton, Solid State Commun. 26, 493 (1978).
[27]G. K. Shenoy, B. D. Dunlap, F. Y. Fradkin, S. K. Sinha, C. W. Kimball, W. Potzel, F. Pröbst, and G. M. Kalvius, Phys. Rev. B 21, 3886 (1980).
[28]H. R. Ott, W. A. Fertig, D. C. Johnston, M. B. Maple, and B. T. Matthias, J. Low Temp. Phys. 33, 159 (1978).
[29]L. P. Woolf, D. C. Johnston, H. B. MacKay, R. W. McCallum, and M. B. Maple, J. Low Temp. Phys. 35, 651 (1979).
[30]L. D. Woolf, M. Tovar, H. C. Hamaker, and M. B. Maple, Phys. Lett. 74A, 363 (1979).
[31]S. K. Sinha, H. A. Mook, D. G. Hinks, and G. W. Crabtree, Bull. Am. Phys. Soc. 26, 277 (1981); S. K. Sinha, G. W. Crabtree, D. G. Hinks, and H. Mook, Phys. Rev. Lett. 48, 950 (1982).
[32]D. E. Moncton, J. Appl. Phys. 50, 1880 (1979).
[33]J. W. Lynn, G. Shirane, W. Thomlinson, R. N. Shelton, and D. E. Moncton, Phys. Rev. B 24, 3817 (1981); J. W. Lynn, in *Ternary Superconductors,* edited by G. K. Shenoy, B. D. Dunlap, and F. Y. Fradkin (North-Holland, Amsterdam, 1981), p. 51.
[34]F. Mancini, R. Teshima, and H. Umezawa, Solid State Commun. 24, 561 (1977).
[35]H. Matsumoto, H. Umezawa, and M. Tachiki, Phys. Rev. B 25, 6633 (1982).
[36]H. Adrian, K. Muller, and Salmann-Ischenko, Phys. Rev. B 22, 4424 (1980).
[37]H. S. Greenside, E. I. Blount, and C. M. Varma, Phys. Rev. Lett. 46, 49 (1981).